Journal Pre-proof

Improvement of Punching Shear Strength of Reinforced Lightweight Concrete Flat Slab using Different Strengthening Techniques

Mohamed Said, Maher A. Adam, Alaa E. Arafa, Ahmed Moatasem

PII: S2352-7102(20)33382-9

DOI: https://doi.org/10.1016/j.jobe.2020.101749

Reference: JOBE 101749

To appear in: *Journal of Building Engineering*

Received Date: 14 February 2020

Revised Date: 21 July 2020

Accepted Date: 11 August 2020

Please cite this article as: M. Said, M.A. Adam, A.E. Arafa, A. Moatasem, Improvement of Punching Shear Strength of Reinforced Lightweight Concrete Flat Slab using Different Strengthening Techniques, *Journal of Building Engineering*, https://doi.org/10.1016/j.jobe.2020.101749.

This is a PDF file of an article that has undergone enhancements after acceptance, such as the addition of a cover page and metadata, and formatting for readability, but it is not yet the definitive version of record. This version will undergo additional copyediting, typesetting and review before it is published in its final form, but we are providing this version to give early visibility of the article. Please note that, during the production process, errors may be discovered which could affect the content, and all legal disclaimers that apply to the journal pertain.

© 2020 Elsevier Ltd. All rights reserved.

Journal Pre-proof

CRediT authorship contribution statement

Mohamed Said: Conceptualization, Software, Validation, Formal analysis, Investigation, Resources, Data curation, Writing – original draft, Writing - review & editing, Visualization, Supervision, Project administration.

Maher A. Adam: Conceptualization, Software, Validation, Formal analysis, Investigation, Resources, Data curation, Writing - review & editing, Visualization, Supervision, Project administration.

Alaa E. Arafa: Conceptualization, Software, Validation, Formal analysis, Data curation, Visualization, Supervision, Project administration.

Ahmed Moatasem: Software, Validation, Formal analysis, Investigation, Resources, Data curation, Funding acquisition.

Journal Pre-proof

Journal Pre-proof

Improvement of Punching Shear Strength of Reinforced Lightweight Concrete Flat Slab using Different Strengthening Techniques

By

Mohamed Said[*1], Maher A. Adam[2], Alaa E. Arafa[3], Ahmed Moatasem[4]

*Corresponding author. Tel: +201007284649, E-mail: mohamed.abdelghaffar@feng.bu.edu.eg

1 Associate Professor, Faculty of Engineering (Shoubra), Benha University, Egypt (E-mail:mohamed.abdelghaffar@feng.bu.edu.eg)
2 Professor, Faculty of Engineering (Shoubra), Benha University, Egypt (E-mail: maher.adam@feng.bu.edu.eg)
3 Professor, National Housing and Building Research Centre (HBRC), Cairo, Egypt
4 Demonstrator, Pyramids Higher Institute for Engineering and Technology, Giza, Egypt

Abstract

This paper investigates the strengthening techniques of lightweight concrete (LWC) flat slabs vulnerable to punching shear failure. Thirteen reinforced LWC flat slab specimens were experimentally tested. The main investigated parameters were the type of shear reinforcement (steel bars, high strength bolts, or glass fiber reinforced polymers (GFRP) rods), spacing, shear reinforcement configuration around the column and the fixation method of shear reinforcement. The test results showed that using radial shear reinforcement with spacing of (d/2) resulted in the most efficient strengthening technique. The punching shear capacities were improved by 77%, 61% and 54% by using steel bars, glass fiber rods and high strength bolts, respectively, compared to the reference specimen. Moreover, using high strength steel bolts fixed to the slabs with steel plates showed the highest ductility compared with the other strengthening techniques Also, the failure mode converted from being brittle shear failure to flexural-shear mode. Non-linear finite element analysis (NLFEA) was carried out for the numerical verification. The analysis adequately reflected the trend of experimental results. Finally, the experimental test results were evaluated with the codes equations. The evaluation showed that ACI 318-2018 code underestimated the punching shear capacity of the tested specimens. On the other hand, Euro Code showed good prediction of the punching shear strength of the tested slabs.

Keywords: Punching shear strength; strengthening; lightweight concrete; flat slabs; NLFEA.

Journal Pre-proof

1. Introduction

In the beginning of the 21st century, studies for the punching shear strength of reinforced concrete (RC) flat slabs supported by columns were conducted by many researchers [1-2]. Decreasing the weight of RC slabs considered as an effective way to solve the slab-column connection problem. The punching shear strength depends on the length of the slab, rather than the thickness of slab [3]. Recently, concrete technology has undergone rapid development, resulting in the production of a new concept of foam concrete [4-5]. The use of foam as a type of admixture for RC is a significant development in the structural construction industry. It led to the innovation of a new type of concrete called lightweight concrete (LWC). LWC is a type of concrete characterized by light self-weight, self-compacting and self-leveling. The mechanical properties of LWC were established by several researchers [6-10]. The proposed compressive strength, elastic modulus and peak strain of LWC were studied by Cui et al. [6]. Also, the thermal properties and shrinkage predictions of LWC were investigated [7-9]. Moreover, Chung et al. [10] evaluated the void distribution and the stiffness of LWC. The results revealed that LWC improved thermal and sound insulation properties while maintaining adequate strength. On the other hand, comparing with normal weight concrete, higher creep, shrinkage, large deflection and lower splitting tensile strength were observed [9]. As an alternative reinforcing material to the steel reinforcement, fiber-reinforced polymer (FRP) bars are considered due to their corrosion resistance characteristic, so the FRP bars have received considerable attention. FRP also has a high strength-to-weight ratio. Therefore, if the FRP system is used to strengthen LWC slabs subjected to punching shear some advantages could be expected.

An investigation of LWC structures reinforced with the different reinforcement system was studied [11-18]. Khaleel et al. [11] studied the efficiency of using FRP systems to strengthen the

Journal Pre-proof

slab-column connection subjected to punching shear. An external FRP stirrup made from glass and carbon fibers were used as a strengthening system. The test results showed that using steel links, GFRP stirrups and CFRP stirrups enhanced the initial cracking load and the load-carrying capacity compared with the control specimens. Moreover, the surface failure of the tested specimens forms a nearly square shape with tension slab side. The sudden collapse of the slabs due to punching failure was prevented for specimens strengthened with L-CFRP laminate [12]. Wiater and Siwowski [13] showed that, the deflection of LWC slabs was significantly larger with comparison to the NWC slabs. Zaher et al. [15] investigated the punching shear behavior of nine half-scale LWC Slabs. LWC was obtained by using polystyrene foam as a partial aggregate replacement to reduce the weight of concrete from 24.0 KN/m3 to 18.5 KN/m3. The test results showed the degradation punching shear performance of LWC slabs when compared with RC slabs. These degradations of LWC specimens were most pronounced in the post-cracking stage until failure. The punching failure of slabs is highly affected by types LWA used in the slabs [16].

The punching shear performance of steel fiber LWC slabs was studied by Caratelli et al. [17]. Three full-scale slab simulating bridge decks were tested. The test results showed that the use of steel fiber LWC appeared as an effective solution for increasing the punching resistance of typical bridge decks. Urban et al. [18] investigated the efficiency of double-headed studs shear reinforcement in LWC flat slabs. The studied parameters included the longitudinal reinforcement ratio and the cross-section of punching shear reinforcement dual headed studs. Double headed-studs showed significant efficiency in resisting punching shear strength. The load-carrying capacities were improved by a range from 16 to 73 % with reference to the specimens without transverse reinforcement.

Journal Pre-proof

Most of the studies focused on the LWC slabs with high flexural reinforcement ratio to induce the clear punching shear failure [19-**Error! Reference source not found.**]. Superior performance of LWC slabs strengthened with headed shear bars compared to conventional stirrups [20]. The punching shear capacities of HSLW and NSLW concrete slabs were tested under eccentric load was nearly similar [21]. Aghayari et al. [22] investigated the improvement of the punching shear strength of RC slabs by FRP and steel sheets. The enhancement in the ultimate capacity of specimens strengthened with steel sheets was more than specimens strengthened with CFRP or GFRP sheets. Lapi et al. [23] pointed out that the shear strength and ductility increased for slab strengthened with post-installed shear reinforcement. El-Kashif et al. [24] investigate experimentally the punching shear behavior of flat slabs-column connections strengthened with CFRP string having a fan shape as a new strengthening technique. The results showed that the proposed strengthening technique improved the punching shear capacity and enhanced the ductility of the flat slabs column connections. Silva et al. [25] indicated that the skewed placement of CFRP at the shear critical area is effective than that of orthogonal placement in the presence of end anchorage. More than 46% of punching shear capacity can be gained by the external strengthening of slab-column connections with a proper bond arrangement. [26] Introduced an experimental program to overcome the risk of brittle punching shear failure in the column region. The increase in punching capacity for slab by post-installed shear bolts ranged from 28% to nearly 55%. Using steel bolts as shear reinforcement in strengthening slabs against punching failure is effective in preventing sudden punching shear failure in flat slabs [27]. The experimental results of strengthened slabs with CFRP system was pointed out that the length of radial cracks was reduced [28-29]. The brittle failure of strengthened slab using shear bolts technique was improved to ductile failure [30]. Flat slab

Journal Pre-proof

strengthened with different types of shear reinforcement was analyzed using NLFEA [31-33]. The mentioned previous research works were focused on normal weight RC flat slabs only. Accordingly, investigation of different techniques for strengthening of LWC flat slabs subjected to punching shear is required.

This paper aims to introduce several strengthening techniques of LWC flat slabs subjected to punching shear. Thirteen specimens of LWC flat slabs were tested. The specimens were perforated in the strengthening places. The main key parameters were the type of shear reinforcement (steel or GFRP), dimensions and layout configuration of shear reinforcement around the column and the fixation method of shear reinforcement (adhesion or fixation of steel bolts using steel plates on each side of the slab). The cracking load, maximum load and load-deflection curves were discussed. In addition, the load- shear studs strain curves were presented. Moreover, the crack pattern and failure modes were observed. NLFEA was performed to simulate the tested LWC flat slabs. ANSYS software [34] was used to develop the models. Finally, the test results were evaluated by the design equations as recommended by different international codes; ACI-318-18 [35], CSA A23.3-2004 [36], ECP-203-2017 [37], BS-8110-1997 [38] and EC-2- EN 1992-1-1 [39].

2. Experimental Program

2.1. Test Specimen Design

The experimental program consists of thirteen specimens of LWC flat slabs with constant plan dimension of 1150 x 1150 mm, thickness (t_s) of 150 mm and effective depth (d) of 130 mm. For all specimens steel reinforcement bars were used in reinforcing the LWC slabs; 16 mm diameter @ 125 mm c/c spacing were used as bottom reinforcement mesh while, 10 mm diameter @ 150

Journal Pre-proof

mm c/c spacing were used as top reinforcement mesh. The specimens were perforated in the strengthening places. The investigated parameters included the type of shear reinforcement (steel or GFRP) bars, dimensions and shear reinforcement layout configuration around the column and also, the fixation method of shear reinforcement (adhesion or fixation of steel bolts using steel plates on each side of the slab). The specimens were divided into three Groups A, B and Group C in addition to control specimen labeled as S1 for comparison. Group A consists of four specimens (S2, S3, S4 and S5) of reinforced LWC flat slabs strengthened with steel bars adhesive with epoxy. Specimens S2 and S3 were strengthened in orthogonal shape with spacing 65 mm (0.5 d) and 130 mm (d) respectively. Also, specimens S4 and S5 were strengthened in a radial shape with spacing 65 mm and 130 mm respectively. The specimens of Group B (S6, S7, S8, and S9) were similar to Group A but GFRP rods adhesive with epoxy were used for strengthening the reinforced LWC slabs. The strengthening technique used for reinforced LWC slabs of Group C (S10, S11, S12 and S13) were steel bolts assembled by steel plate on each side of the slab. Specimens S10 and S11 were strengthened in orthogonal shape while, specimens S12 and S13 were strengthened in a radial shape. The load plate dimensions that represented the column was set to be 150*150*60 mm co-centered with the specimen. Table 1 demonstrated the main parameters for the specimens. Also, the reinforcement details of the control specimen S1, Groups (A, B) and Group C are shown Figs 1, 2 and 3, respectively. The different strengthening techniques was used in the manuscript were applicable to be used in the existing structure.

Journal Pre-proof

Journal Pre-proof

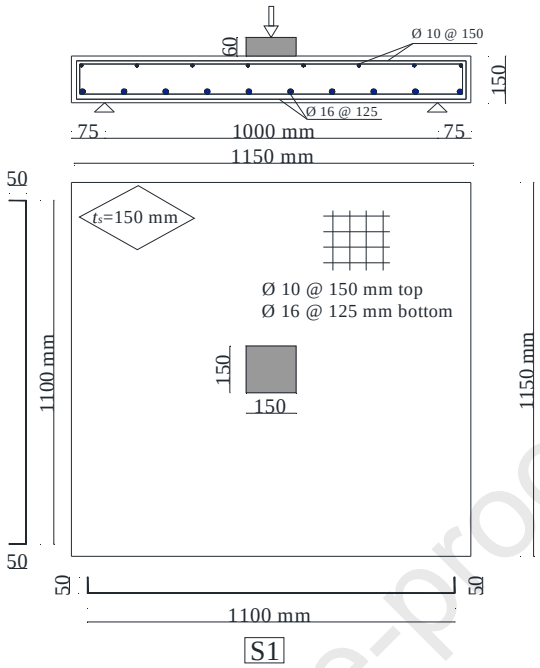

Fig. 1 Control Specimen S1

Journal Pre-proof

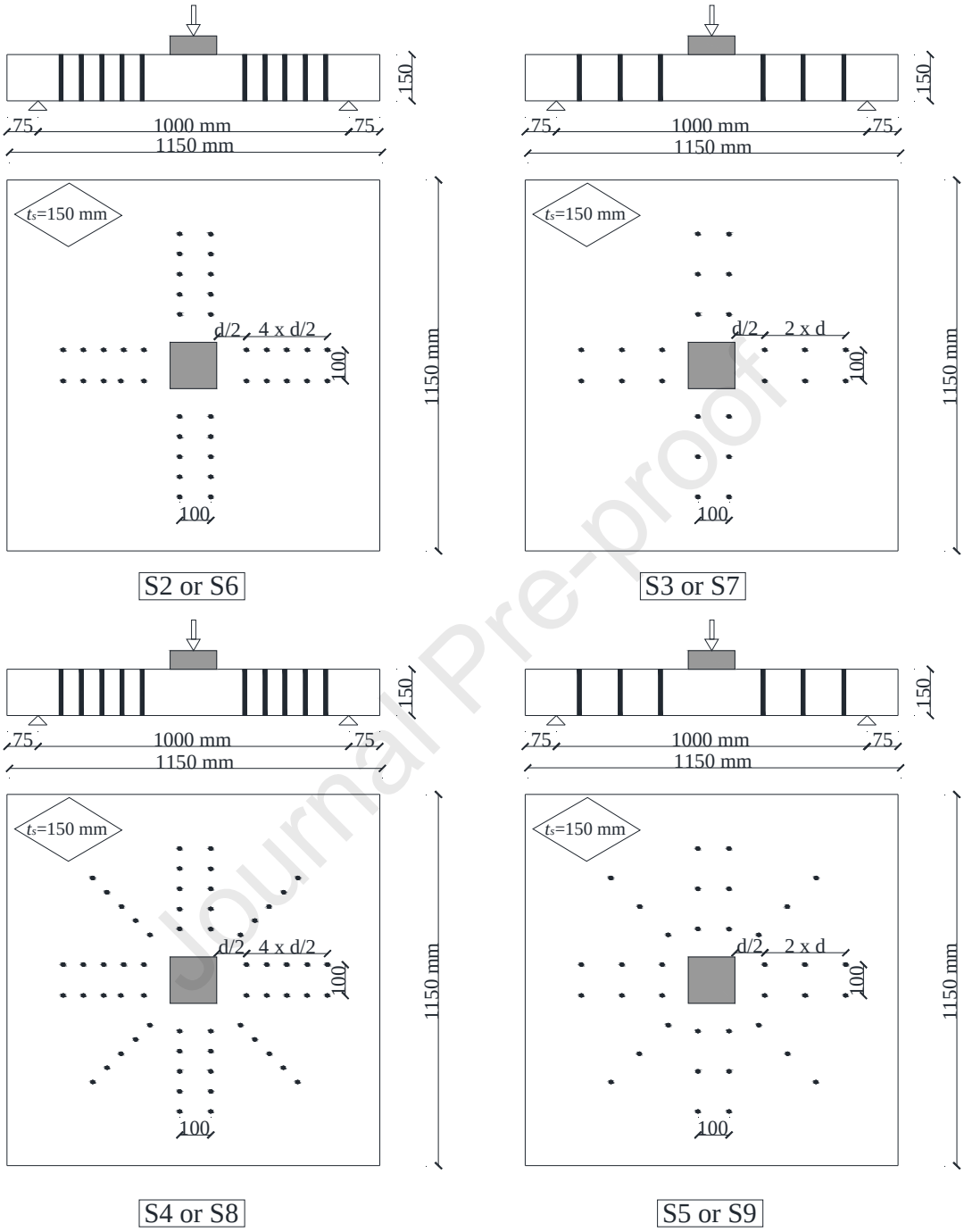

Fig. 2 Group A and B Specimens

Journal Pre-proof

Journal Pre-proof

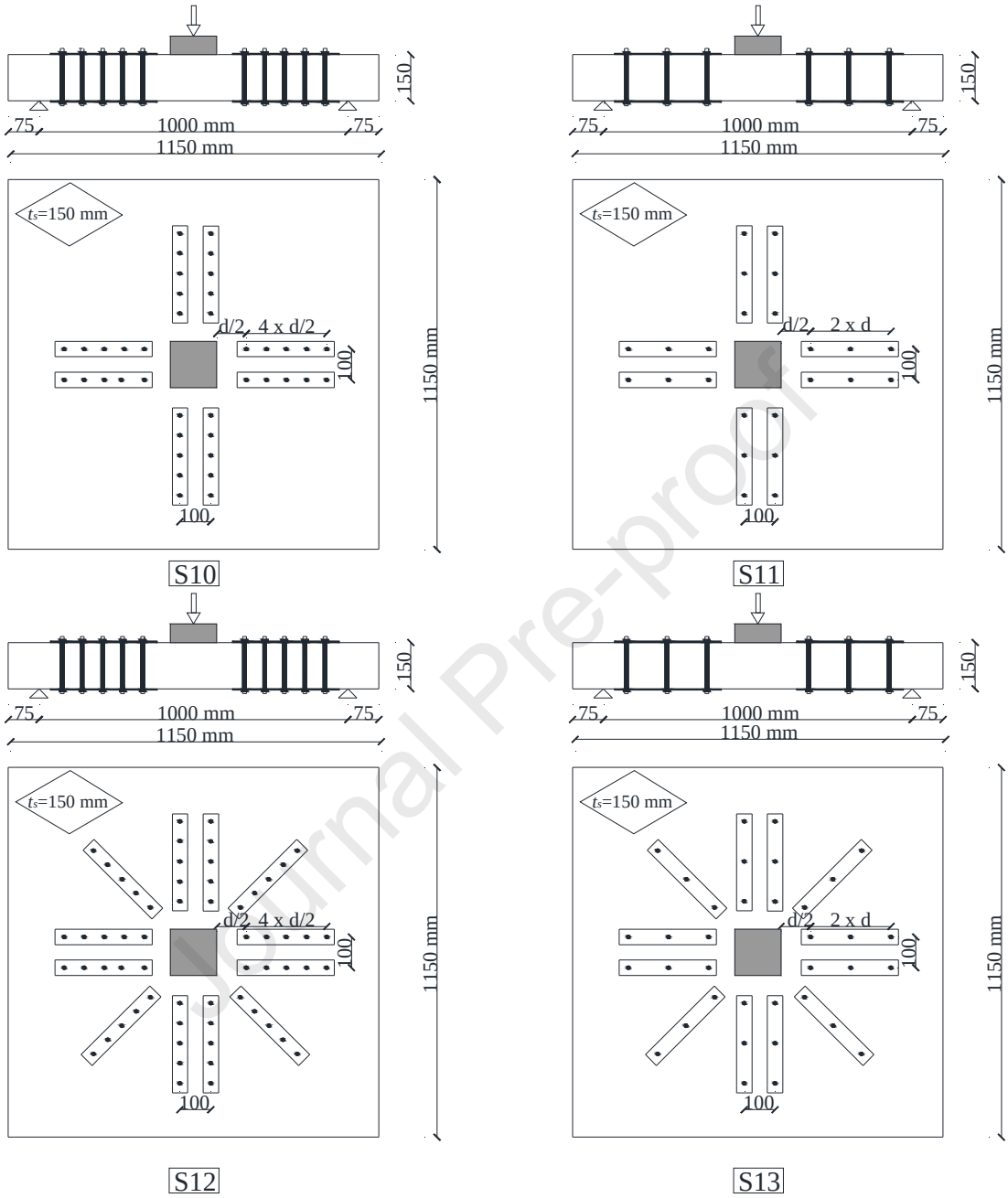

Fig. 3 Group C Specimens

Table 1: Test Specimens Strengthening Techniques Classification

Group	Specimen	Strengthening RFT / S (mm)	Shape	Strengthening Techniques
----	S1	----	Control sample	without shear RFT
Group (A)	S2	ϕ 12 / 65	Orthogonal RFT	steel reinforcement bars fixed with Epoxy
	S3	ϕ 12 / 130		
	S4	ϕ 12 / 65	Radial RFT	
	S5	ϕ 12 / 130		
Group (B)	S6	G 12 / 65	Orthogonal RFT	GFRP rods fixed with Epoxy
	S7	G 12 / 130		
	S8	G 12 / 65	Radial RFT	
	S9	G 12 / 130		
Group (C)	S10	bolt ϕ 12 / 65	Orthogonal RFT	High strength steel bolts with steel plate
	S11	bolt ϕ 12 / 130		
	S12	bolt ϕ 12 / 65	Radial RFT	
	S13	bolt ϕ 12 / 130		

Journal Pre-proof

2.2. Materials

The specimens were made of LWC with a density of 16.50 kN/m^3. The mix proportions for meter cubic are given in Table 2. In order to produce homogeneous mixtures, the materials were mixed very well (3 min dry mixing, 2 min wet mixing and 2 min high rate mixing) producing a uniform and flowing mixture. Average density and target mean strength of twelve concrete cubes

were 16.50 KN/m^3 and 25 MPa respectively. The cubic concrete strength was determined by testing 12 cubes 150 x 150 x 150 mm after 28 days of casting.

Table 2: Mix Proportions for Cubic Meter of Concrete

Cement (Kg)	Sand (Kg)	Coarse aggregate (Kg)	Water (Littre)	W/C	Additives (Littre)	Silica fume (Kg)	Foam (Kg)
450	630	630	139	0.308	13.5	40	7.25

GFRP rods of diameter 12 mm were used as shear reinforcement. The bars had a helical wire wrapping to enhance the bond between the bars and the surrounding concrete. The elastic modulus of GFRP bars was 55 GPa while the ultimate strength and strain were 800 MPa and 2.1% respectively as given by the manufacturer. In addition, deformed high tensile steel reinforcement bars of 10 mm, 12 mm, and 16 mm diameter with yield strength of 400 MPa and ultimate strength of 580 MPa were used.

2.3. Test Setup

Fig. 4 presents the test setup for all specimens. The load was applied at a stroke-controlled rate of 0.2 mm/min. The deflection of the specimens was monitored using three linear variable differential transducers (LVDT); the first was set as the mid span of the slab, the second was set at 150 mm from the first (opposite to loading plate face) and the third was set at 150 mm from the second. The strains of the shear studs were measured using strain gauge as shown in Fig. 5.

Journal Pre-proof

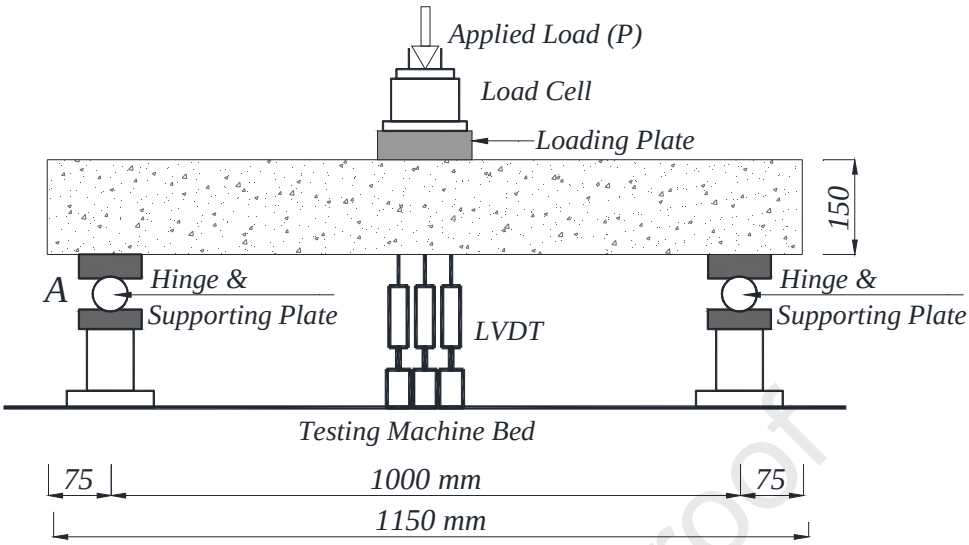

(a)

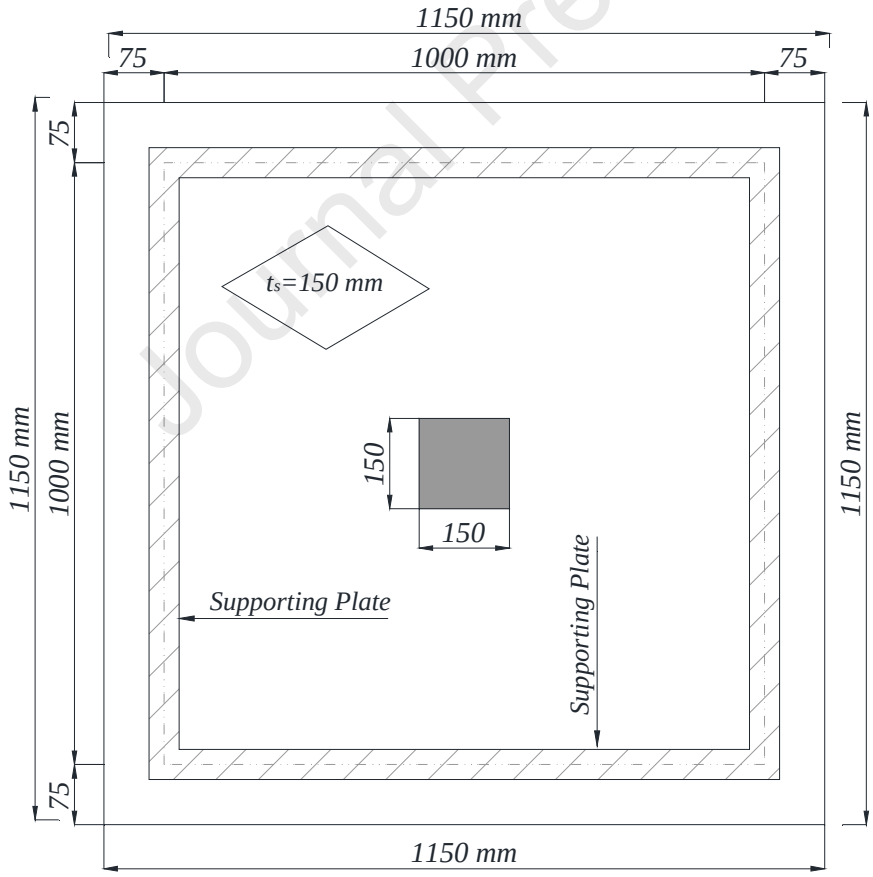

(b)

Journal Pre-proof

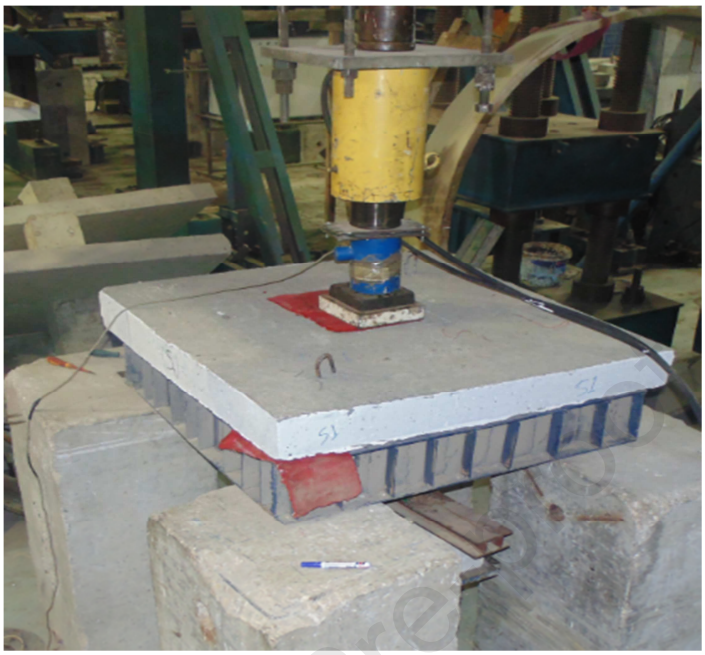

(c)

Fig.4 Test Setup of the Slab

Fig. 5 Attached Strain Gauge to the Reinforcement Bars

Journal Pre-proof

3. Test Results and Discussion

The enhancement in the punching shear strength of the reinforced LWC slabs using several techniques was discussed in terms of cracking pattern, cracking load, load-deflection behavior and also, the developed strain in the shear studs.

3.1. Cracking Load and Ultimate Load

All specimens were visually observed till the appearance of the first crack with the recording of the corresponding first crack load. Figure 6 shows the crack pattern for all tested specimens. Also, Table 3 summarizes the observed test results. For the reference specimen S1, the first crack load (P_{cr}) appeared at 75 KN and failed at a load of 340 KN. The crack pattern propagation showed very fine tangential cracks that were first observed around the loading plate, and then few fine cracks started in radial directions running from the loading plate faces toward the slab edges.

Comparing with the control specimen S1, no significant change in the first cracking load (P_{cr}) was observed for all specimens. On the other hand, using different strengthening techniques showed different enhancement levels in the load-carrying capacity (P_u). For Group A, using steel bars as strengthening techniques improved the load-carrying capacity for S2, S3, S4 and S5 by 70%, 54%, 77% and 59%, respectively. Also, the inclusion of GFRP shear reinforcement for strengthening Group B enhanced the load-carrying capacity compared with the control specimen S1. At the ultimate level, the load-carrying capacity was improved for S6, S7, S8 and S9 by 52%, 41%, 61% and 48%. The enhancement levels were less than Group A due to the low stiffness and modulus of elasticity of GFRP bars compared to steel bars. For Group C, the use of high strength steel bolts as shear reinforcement for specimens S10, S11, S12 and S13 enhanced the

Journal Pre-proof

load carrying capacity by 39%, 21%, 54% and 40%, respectively. Comparison of results demonstrates that the all different strengthening techniques system had an insignificant effect on the cracking loads. The largest effect on the ultimate capacity for specimens strengthened with shear steel link. Provision of shear links in radial direction led to maximum enhancement in the ultimate capacity. The perimeter of the cracking was increased with increasing the shear links.

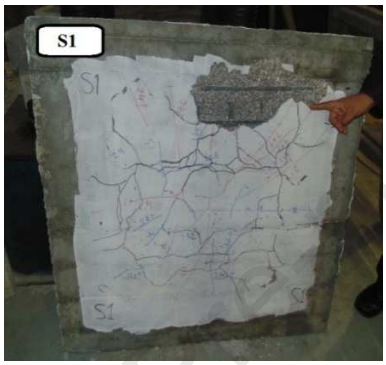

S1

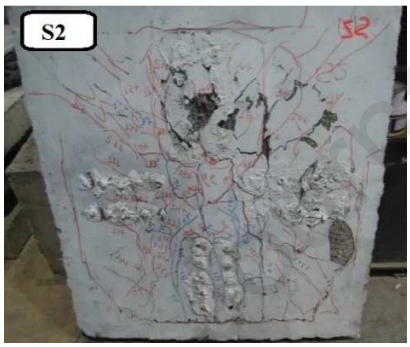

S2

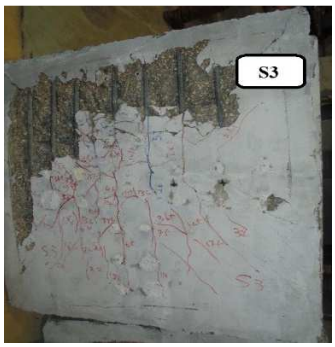

S3

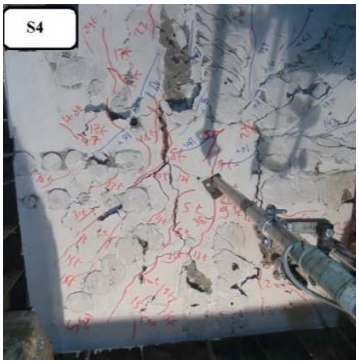

S4

S5

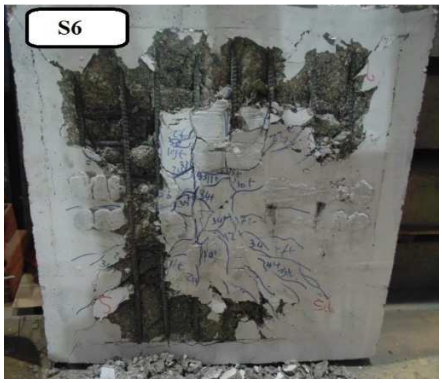

S6

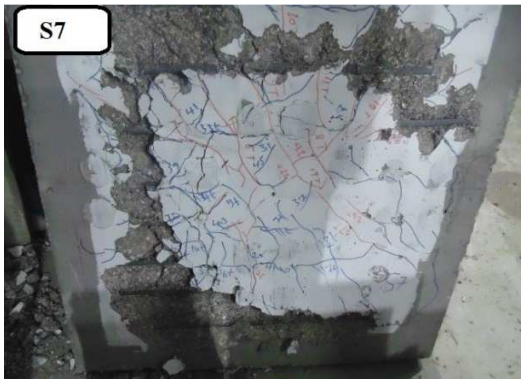

S7

S8

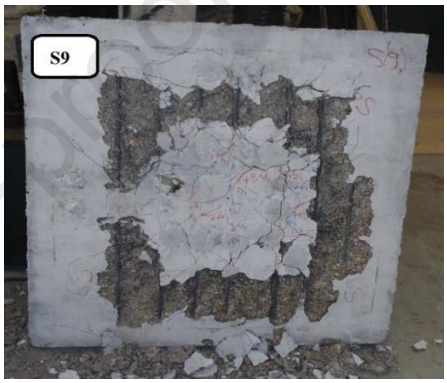

S9

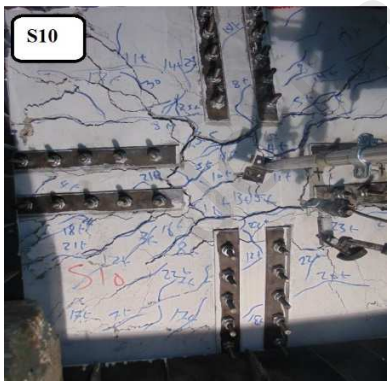

S10

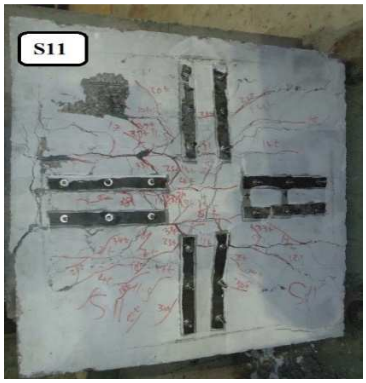

S11

Journal Pre-proof

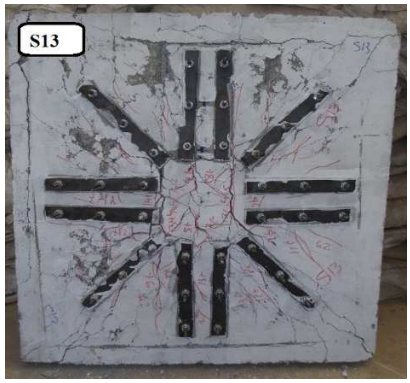

S12 **S13**

Fig. 6 Cracks Pattern for the Tested Specimens

3.2. Load-Deflection Curves

The experimental load-deflection curves for Groups A, B, and Group C are plotted in Figs.7, 8 and 9, respectively. For the control specimen S1, the pre-peak load-deflection relationship was almost linear response up to the peak load. The absence of nonlinear stage before failure was observed hence no ductility for the specimen was gained. For Group A, the load-deflection curves showed the same behavior at the pre-peak load for specimen S1. Provision of steel shear reinforcement showed an enhancement in the post-peak stage for the tested specimens. The load-deflection relationship for Group B had the same trend for Group A. Generally, using GFRP rods as shear reinforcement had a significant effect in post-cracking behavior. The specimens of Group C which strengthened by high strength steel bolts fixed to the slabs with steel plates had a more ductile behavior compared with the other specimens. A noticeable enhancement in the maximum deflection and more ductile behavior was observed by the long plateau developed after the peak load. Increasing the spacing between the strengthening rods from d/2 to 2d remarkably decreased the effectiveness of the strengthening measure for all groups. Based on the plotted load-deflection curves, the following measurements can be evaluated as follows:

Journal Pre-proof

Journal Pre-proof

a. Ductility Factor and Energy Absorption

The ductility factor (*DF*) can be defined as the ratio of the ultimate deformation to the deformation at the beginning of the horizontal path. The energy absorption (*I*) can be defined as the area under the load-deflection curve. The values of (*DF*) and (*I*) for all specimens were recorded in Table 4. The inclusion of shear reinforcement, improved the ductility factor comparing with the control specimen S1. For Group A, using steel bars as shear reinforcement enhanced the ductility factor for S2, S3, S4, and S5 by 28%, 16%, 57% and 45% respectively. In addition, for Group B, using GFRP rods as shear reinforcement improved the ductility factor for S6, S7, S8, and S9 by 8%, 7%, 8% and 10% respectively. Moreover, for Group C, using high strength steel bolts with steel plates as shear reinforcement showed a significant enhancement in the ductility factor, *DF* for S10, S11, S12, and S13 was improved by 167%, 313%, 202% and 231%, respectively.

Based on the comparison between the specimens, it can be concluded that the strengthening techniques for the specimens of Group A have more effective enhancement of punching shear strength capacity Pu compared with Group B and Group C. Generally, using a radial reinforcement spaced with 0.5 d (65 mm) was the most efficient strengthening technique to enhance the punching shear strength of LWC flat slabs. All specimens of group A almost have the same failure behavior due to the brittle and sudden failure (punching shear failure). On the other hand, a noticeable ductile behavior after peak load was observed in Group C. Moreover, strengthening reinforced LWC flat slab with high strength bolts with steel plates at spacing d/2 change failure mode from being a sudden failure to shear failure with flexural cracks.

Journal Pre-proof

Journal Pre-proof

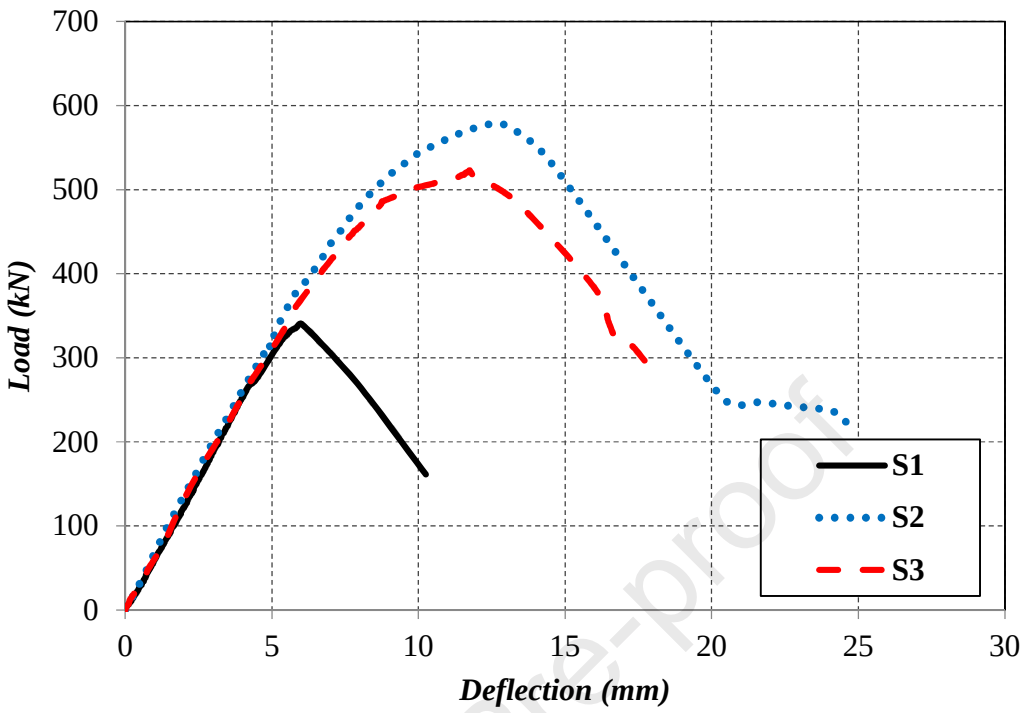

(a)

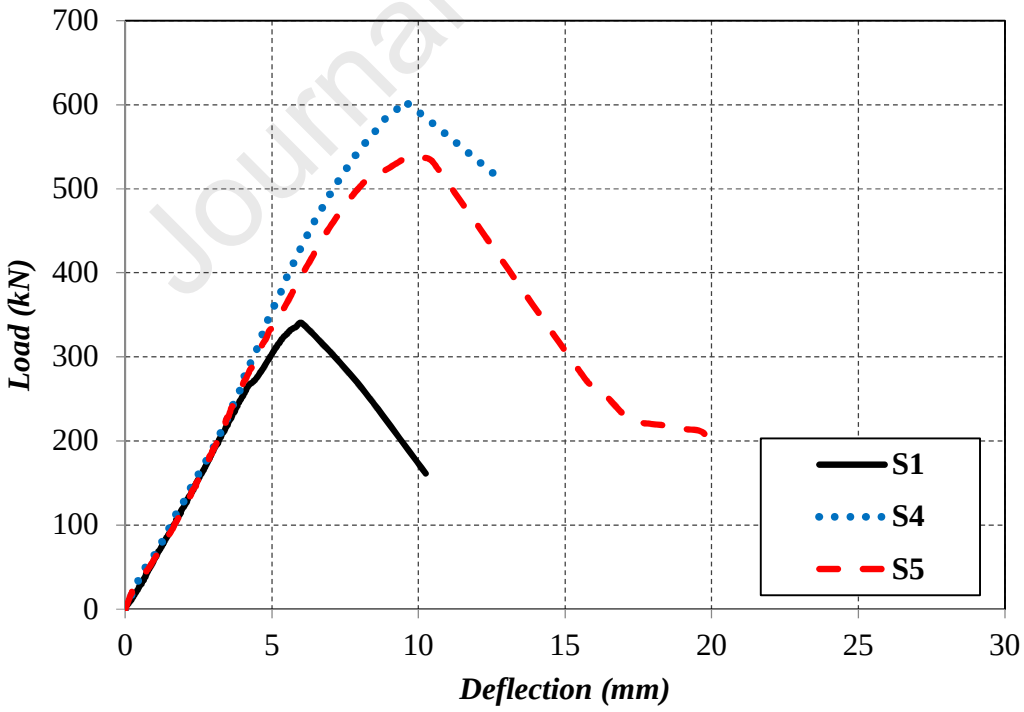

(b)

Fig.7 Load-Deflection Curves of the Tested Specimens of Group A

Journal Pre-proof

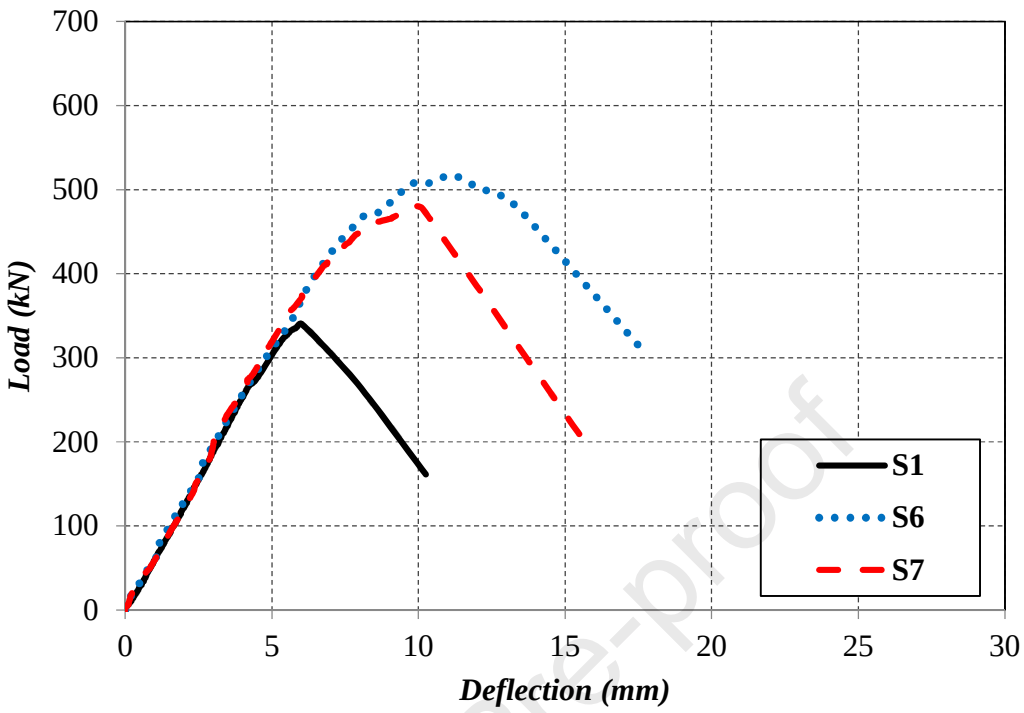

(a)

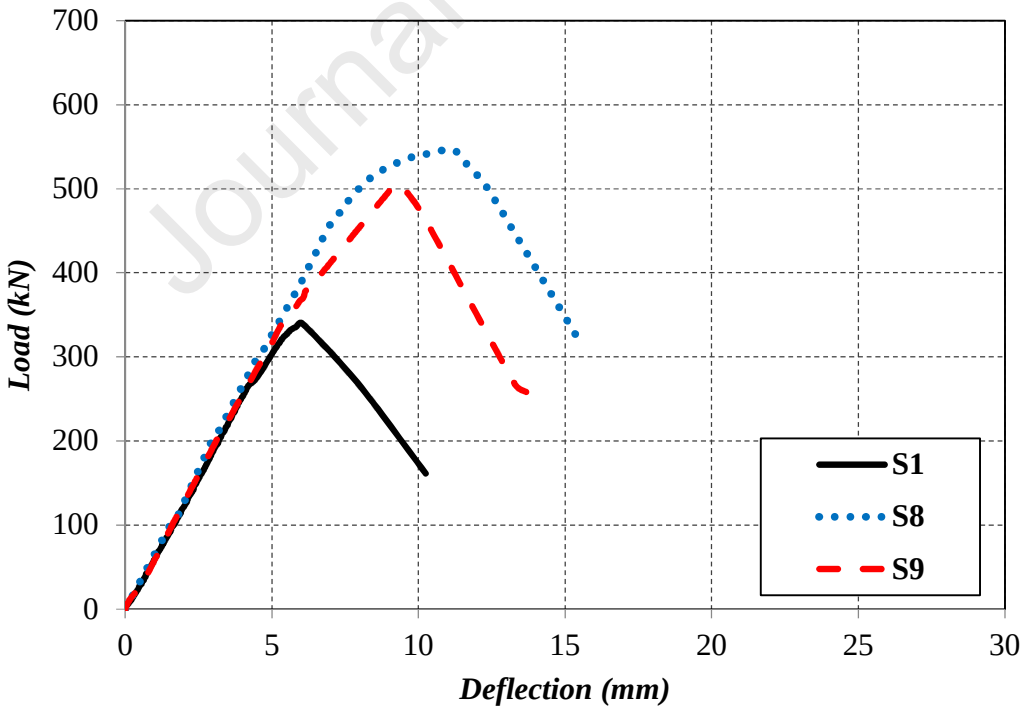

(b)

Fig.8 Load-Deflection Curves of the Tested Specimens of Group B

Journal Pre-proof

Journal Pre-proof

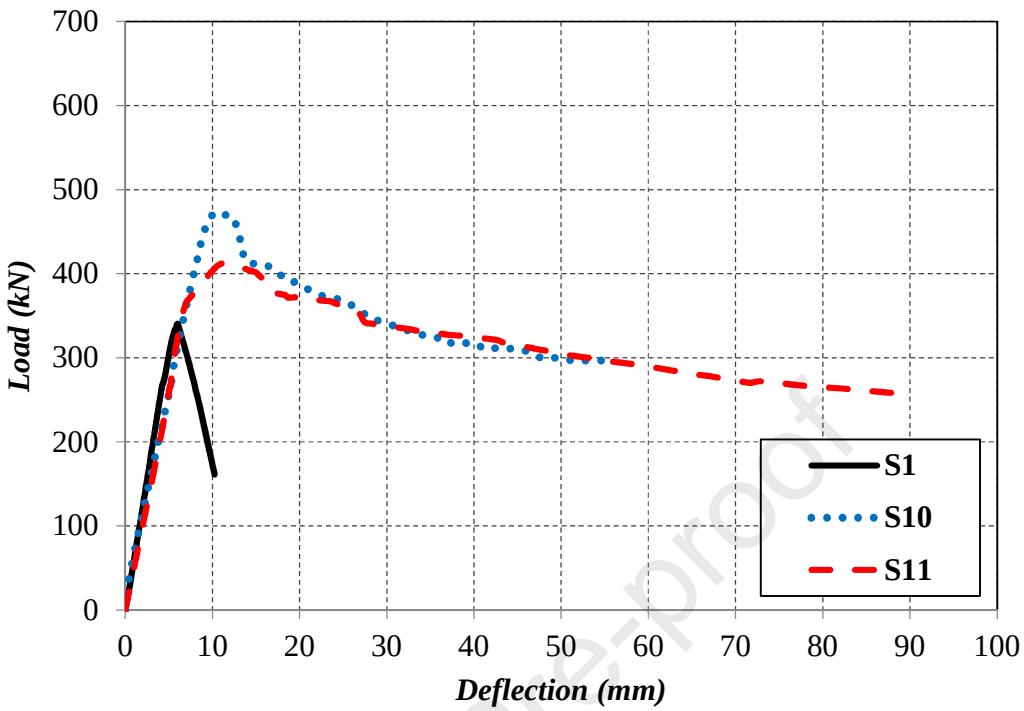

(a)

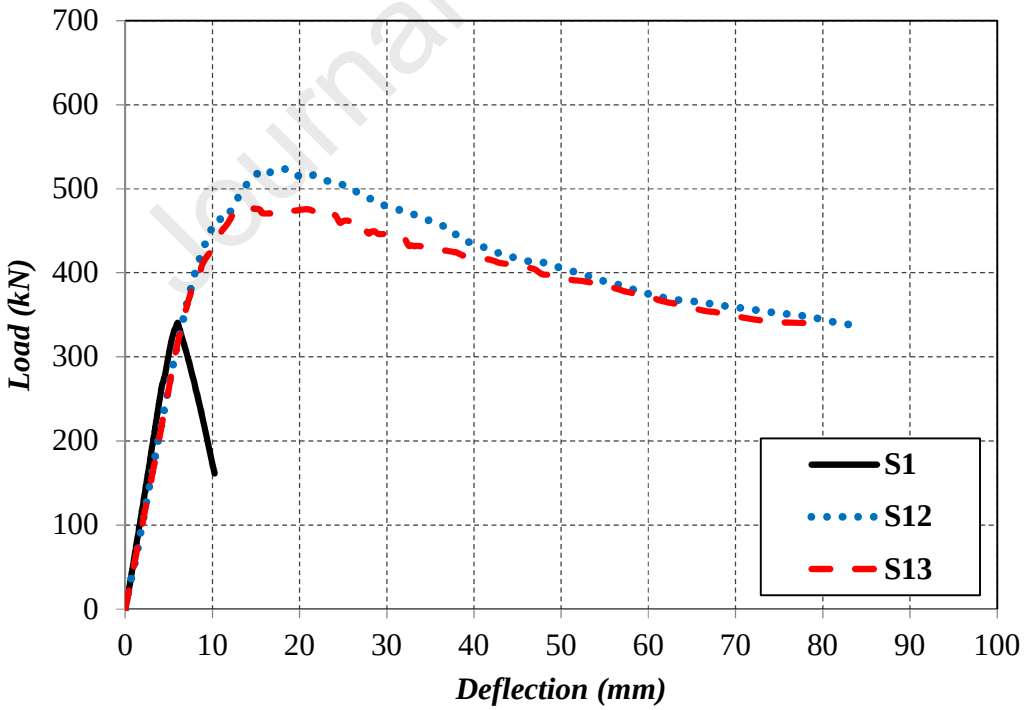

(b)

Fig.9 Load-Deflection Curves of the Tested Specimens of Group C

Journal Pre-proof

Journal Pre-proof

Table 3: Experimental Results of the Tested Specimens

Group	Slab	Experimental Test Results					Relative Experimental Results to the Control Specimen (S1)				
		P_{cr} (kN)	P_u (kN)	δ_u (mm)	DF	I (kN.mm)	$\frac{P_{cr}}{P_{cr-S1}}$	$\frac{P_u}{P_{u-S1}}$	$\frac{\delta_u}{\delta_{u-S1}}$	$\frac{DF}{DF_{S1}}$	$\frac{I}{I_{S1}}$
	S1	75	340	6.03	1.72	2191	1.00	1.00	1.00	1.00	1.00
Group A	**S2**	80	576	13.2	2.2	8960	1.07	1.69	2.15	1.28	4.09
	S3	77	523	11.75	2	6430	1.03	1.54	1.95	1.16	2.93
	S4	85	603	9.95	2.7	5200	1.13	1.77	1.65	1.57	2.37
	S5	81	539	10.50	2.5	6440	1.08	1.59	1.58	1.45	2.93
Group B	**S6**	77	517	11.25	1.85	6320	1.03	1.52	1.87	1.08	2.88
	S7	76	480	10.15	1.84	4840	1.01	1.41	1.68	1.07	2.21
	S8	84	546	11.23	1.86	5650	1.12	1.61	1.86	1.08	2.58
	S9	78	504	9.18	1.9	4260	1.04	1.48	1.52	1.10	1.94
Group C	**S10**	77	473	11.14	4.6	27300	1.03	1.39	1.85	2.67	12.46
	S11	80	412	10.27	7.11	18500	1.07	1.21	1.70	4.13	8.44
	S12	82	522	18.3	5.2	33780	1.09	1.54	3.03	3.02	15.42
	S13	76	476	15.35	5.7	30300	1.01	1.40	2.55	3.31	13.83

Where:

P_{cr} : cracking load of the specimens in (KN);

P_u : ultimate load-carrying capacity in (KN);

δ_u : corresponding deflection for the ultimate load in (mm);

I : energy absorption in (KN.mm);

DF : Ductility factor

3.3. Load-Shear Stud Strain

The maximum strain developed in the shear studs was measured at the first stud opposite to the loading plate. Figs.10, 11 and 12 present the load-shear studs strains for Groups A, B and C respectively as it possible. The strains in studs were comparatively small at cracking. After

cracking, strains increased rapidly with strain hardening until the occurrence of failure. The maximum shear strain values in studs for the tested slabs are recorded in Table 4.

Table 4: Shear Stud Strain of the Tested Specimens

Group	Slab	Shear Stud Strain (ε_s)
Group A	S2	0.00089
	S3	0.00028
	S4	0.00097
	S5	0.00085
Group B	S6	0.003
	S7	0.0023
	S8	0.0012
	S9	0.0024
Group C	S10	0.0018
	S11	0.00145
	S12	0.00062
	S13	0.0038

Journal Pre-proof

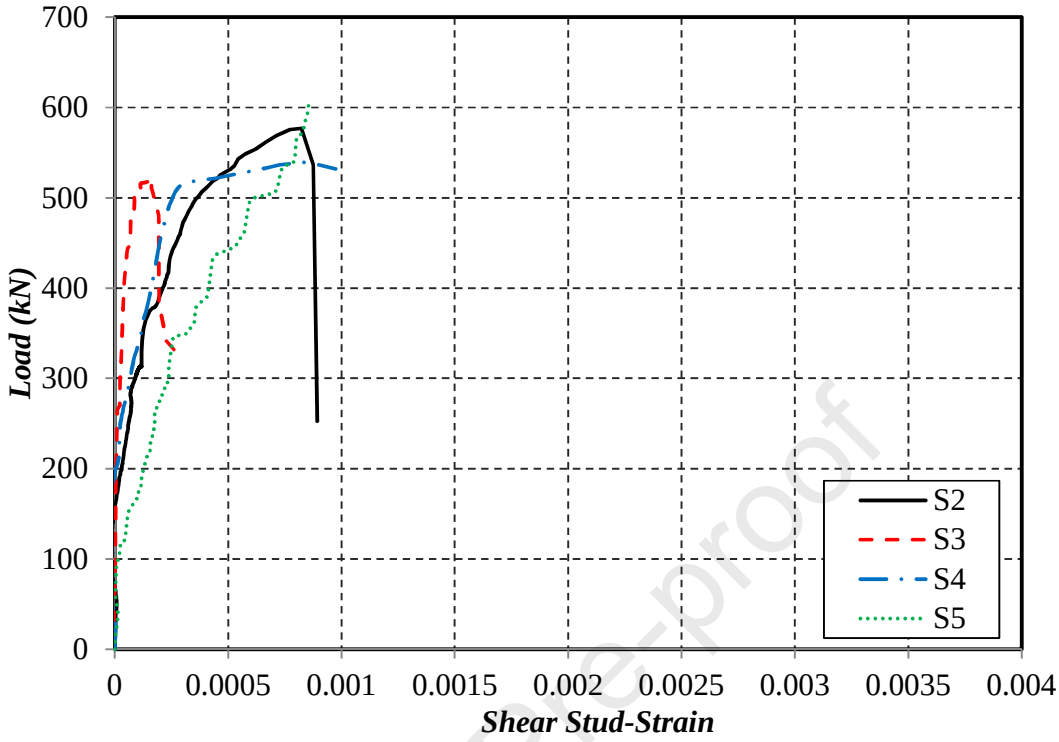

Fig.10 Load-Shear Stud Strain for Group A

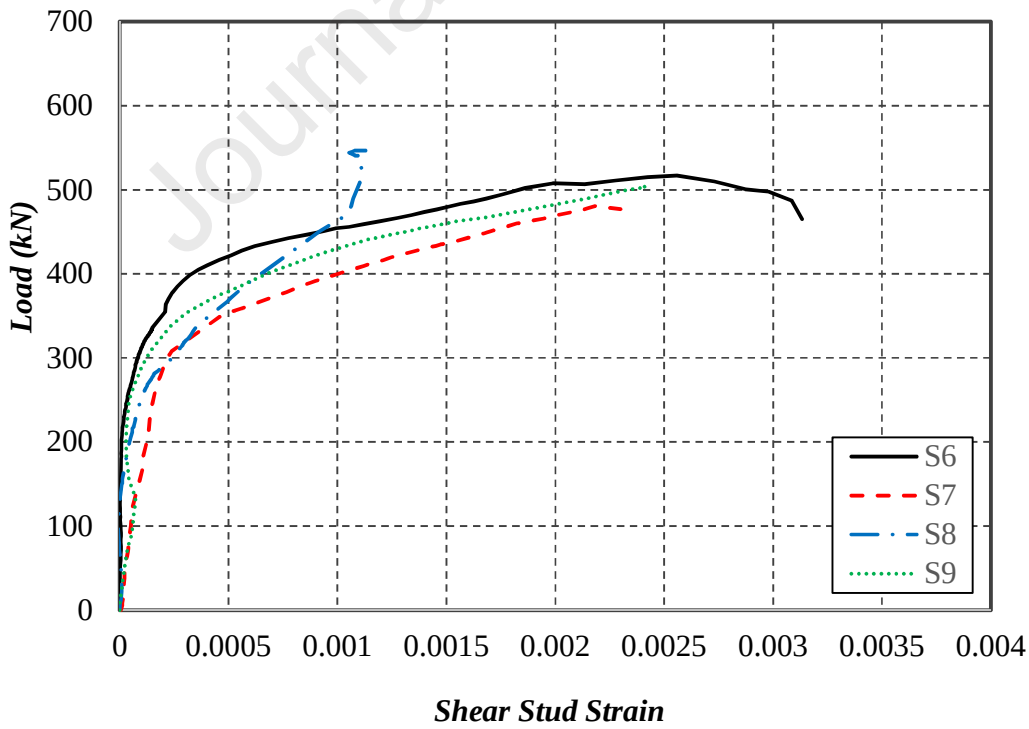

Fig.11 Load-Shear Stud Strain for Group B

Journal Pre-proof

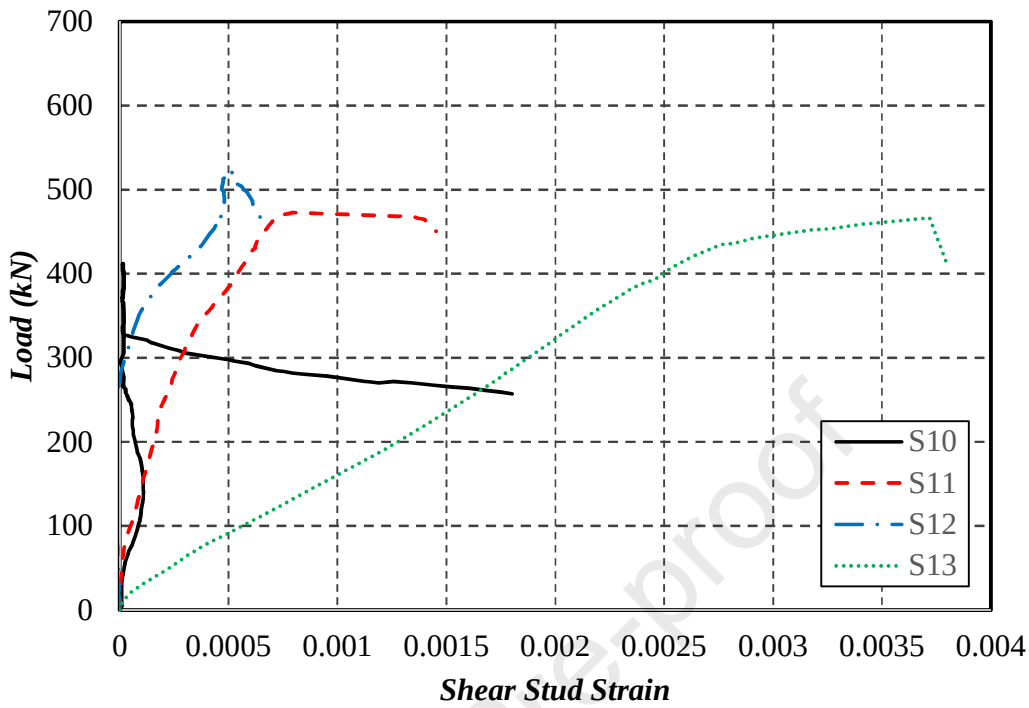

Fig.12 Load-Shear Stud Strain for Group C

4. Non-Linear Finite Elements Analysis (NLFEA)

NLFEA was performed to simulate the tested concrete beams. The commercially well-established finite element analysis software package ANSYS (ANSYS release 15.0) [34] was used. The load-deflection curve is the important aspect in verifying the performance of LWC flat slabs. It includes beneficial parameters such as: the ultimate load (P_u), the corresponding ultimate deflection (δ_u) and the energy absorption (I). Accordingly, comparing the extracted results from the idealized models with the test results considered an efficient method to validate the models.

Journal Pre-proof

4.1. Finite Element Geometric Idealization

The structural element types used for the geometric idealization of the different materials are Solid 65 for concrete as its capability to the plastic deformation, cracking and crushing in three directions. 3-D spar elements (Link 180) were used for idealized reinforcing bars. It has two nodes and three DOF. Also, has the capability of plastic deformation. Solid 45 was idealized at the location of loading and supports in the specimens to avoid stress concentration problems. The structural element types used to discrete the different materials are presented in Fig. 13.

(a) Solid 65 (b) Link 180 (C) Solid 45

Fig.13 Structural Elements Idealization for the Numerical Models [34]

Journal Pre-proof

In order to solve the nonlinear analysis equations of LWC slabs, the Newton-Raphson equilibrium iteration technique is used in the ANSYS software [34]. This technique is based on a series of successive linear approximations with corrections. The convergence criterion is based on a displacement control. In order to improve the convergence of nonlinear analysis, adaptive descend gene, linear searching, forecasting and dichotomy were used at the same time.

The displacement boundary conditions are required to constrain the models. To simulate the hinged support boundary condition of the slabs, the translations at the nodes (U_X, U_Y and U_Z) are

assigned as a constant value of zero. The load is applied as incremental loads. Adjustment is set for each increment to reach results at a certain specific load level. The maximum number of iterations in each load step is set as program default.

4.2. Constitutive Modelling for Concrete in Compression

The constitutive modelling for concrete in compression is adopted by Hognestad-Popvics stress-strain curve [40]. As shown in Fig.14, the curve consists of two branches, the first branch represents the ascending one until the peak stress (f_p) and the corresponding strain (ε_p) are reached. It is defined by:

$$f_{ci} = f_p \left(2\left(\frac{\varepsilon_{ci}}{\varepsilon_p}\right) - \left(\frac{\varepsilon_{ci}}{\varepsilon_p}\right)^2 \right) \tag{1}$$

Where:

f_p = the peak compressive stress; determined experimentally from standard specimens;

ε_p = the concrete compressive strain corresponding to f_p;

f_{ci} = the concrete compressive stress corresponding to concrete compressive strain ε_{ci};

ε_{ci} = the concrete compressive strain corresponding to concrete compressive stress f_{ci}.

The second branch presents the descending branch (post peak) in which the curve descends into a softening region till the ultimate strain (ε_{cu}) and crushing failure occurs. The stress-strain curve for this branch is represented by the following equation [40]:

$$f_{ci} = f_p \frac{n\left(\frac{\varepsilon_{ci}}{\varepsilon_p}\right)}{n - 1 + \left(\frac{\varepsilon_{ci}}{\varepsilon_p}\right)^n} \tag{2}$$

$$n = \left(\frac{E_c}{E_c - E_{Sec}}\right) \tag{3}$$

Where:

E_{sec} = the secant modulus at peak stress in MPa, and is defined as:

$$E_{Sec}=(\frac{f_p}{\varepsilon_p}) \tag{4}$$

E_c = the initial tangent modulus for concrete in MPa, and is defined as according to ACI-318-18 [35] by the following equation:

$$E_c = 4700\sqrt{f_c'} \tag{5}$$

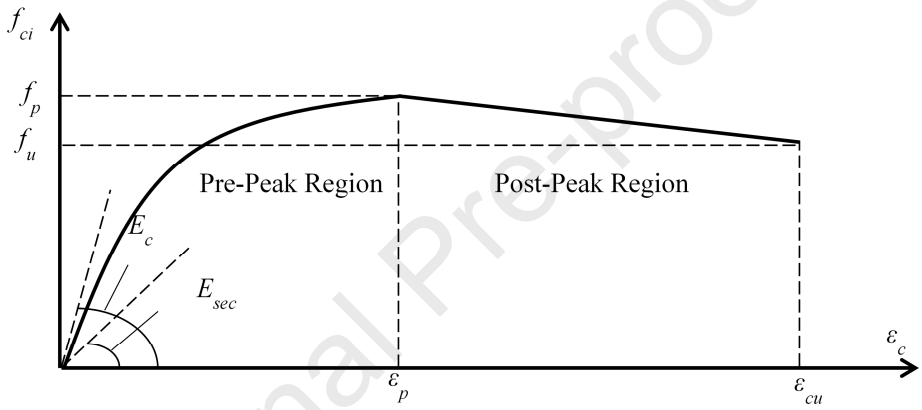

Fig.14 Hognestad-Popvics Stress-Strain Curve for Concrete in Compression [40]

4.3. Constitutive Modelling for Concrete in Tension

The simplified concrete model in tension was used in the simulation of the NLFEA model. Fig.15 presents the uniaxial tensile stress-strain curve for concrete [41]. As shown in the figure, the stress-strain curve is linear till the ultimate tensile strength of concrete (f_{tu}) is reached at corresponding ultimate tensile strain (ε_{tu}). The tensile stress and strain values after the ultimate level equal to zero.

$$f_t = E_c \times \varepsilon_t \qquad 0 \le \varepsilon_t \le \varepsilon_{tu} \tag{6.a}$$

$$f_t = 0 \qquad \varepsilon_t \ge \varepsilon_{tu} \tag{6.b}$$

Journal Pre-proof

Where:

f_t = the tensile strength of reinforced concrete and is assumed as 0.6 $\sqrt{f_c'}$ according to ACI318-18 [35] (in MPa);

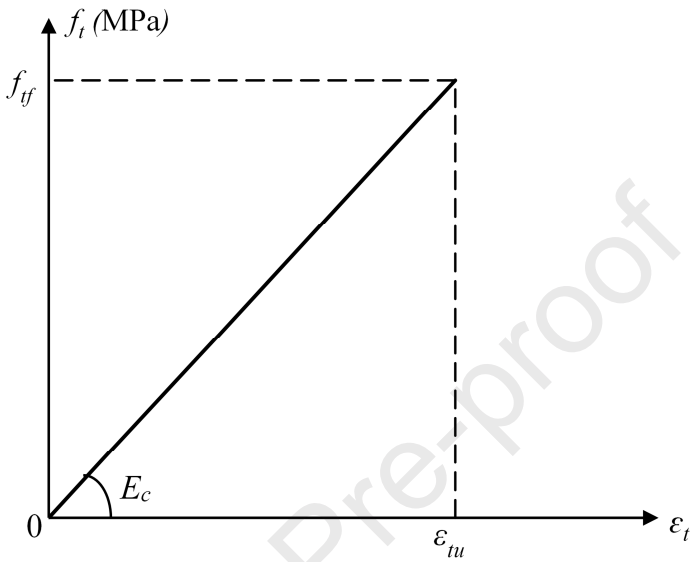

Fig.15 Uniaxial Tensile Stress-Strain Curve for Concrete [41]

In case of the tensile stress of concrete in the principal direction exceeds the tensile strength (f_t), cracks form and tensile failure eventually will occur. In addition, shear and normal stiffness are reduced, consequently the tensile strength of concrete decreases gradually to zero.

4.4. Failure Criteria for Concrete

The criterion for failure of concrete due to a multi-axial stress state can be expressed in the form [34]:

$$\frac{F}{f_c} - S \geq 0 \tag{7}$$

Where:

F = a function of the principal stress state; σ_{xp}, σ_{yp}, σ_{zp};

Journal Pre-proof

S = failure surface expressed in terms of principal stresses and the strength parameters f_{tu}, f_c, f_{cb}, f_{bh} and f_{uh};

f_{tu} = ultimate uniaxial tensile strength;

f_c = ultimate uniaxial compressive strength;

f_{cb} = ultimate biaxial compressive strength;

f_{bh} = ultimate compressive strength for a state of biaxial compression superimposed on hydrostatic stress state;

f_{uh} = ultimate compressive strength for a state of uni-axial compression superimposed on hydrostatic stress state.

In the current research, the stress function by William and Warnke [42] is adopted in which both the failure surface S_f and function F_σ are expressed in terms of principal stresses indicated as, σ_1, σ_2 and σ_3 .

Where:

$\sigma_1 = max(\sigma_{xp}, \sigma_{yp}, \sigma_{zp})$;

$\sigma_3 = min(\sigma_{xp}, \sigma_{yp}, \sigma_{zp})$;

$\sigma_1 \geq \sigma_2 \geq \sigma_3$,

The failure of concrete is categorized into four domains:

a) $0 \geq \sigma_1 \geq \sigma_2 \geq \sigma_3$ (compression - compression - compression)

b) $\sigma_1 \geq 0 \geq \sigma_2 \geq \sigma_3$ (tensile - compression - compression)

c) $\sigma_1 \geq \sigma_2 \geq 0 \geq \sigma_3$ (tensile - tensile - compression)

d) $\sigma_1 \geq \sigma_2 \geq \sigma_3 \geq 0$ (tensile - tensile - tensile)

Journal Pre-proof

Fig. 16 shows the 3-D failure surface in principal stress state [42]. The angle of similarity η represents the relative magnitudes of the principal stresses. Fig. 17 shows also the failure surface for biaxial or nearly biaxial stress states. In case that the principal stresses in (σ_{xp}) and (σ_{yp}) are non-zero, then the three surfaces exhibited for (σ_{zp}) are for (σ_{zp}) equal to zero, (σ_{zp}) slightly less than zero, and (σ_{zp}) slightly greater than zero. The mode of failure for the material depends on the sign of (σ_{zp}). For simplicity, in case of both (σ_{xp}) and (σ_{yp}) are negative and (σ_{zp}) is slightly positive, cracking would be predicted in a direction perpendicular to the (σ_{zp}) direction. However, in case of (σ_{zp}) is slightly negative or zero, the material is assumed to be crushed.

Input strength parameters f_{tu}, f_c, f_{cb}, f_{bh} and f_{uh} are needed to define the failure surface as well as an ambient hydrostatic stress state. The ultimate uniaxial compressive strength f_c, was taken based on test results of cylindrical and cube concrete samples for each element, and f_{tu} was taken as recommended by ACI specifications, ($f_{tu} = 0.1\ f_c$). The other parameters were taken as:

$$f_{cb} = 1.2\, f_c\ , f_{bh} = 1.45\, f_c, and\ f_{uh} = 1.725\, f_c \tag{8}$$

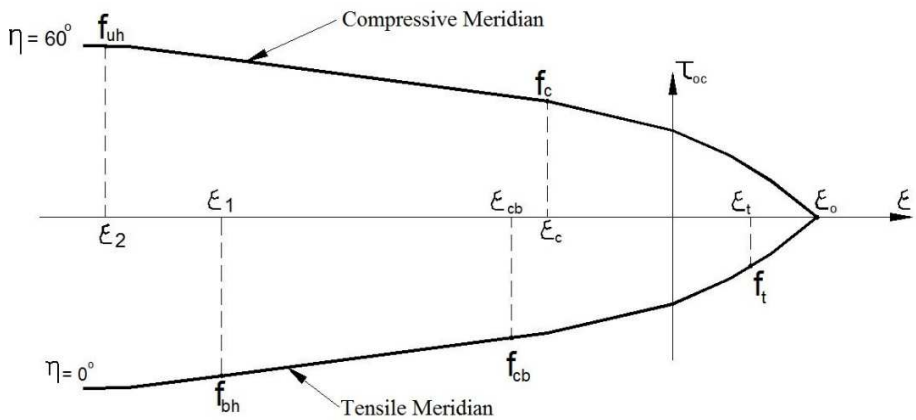

Fig.16 Failure Surface of Concrete in Principal Stress Space [42]

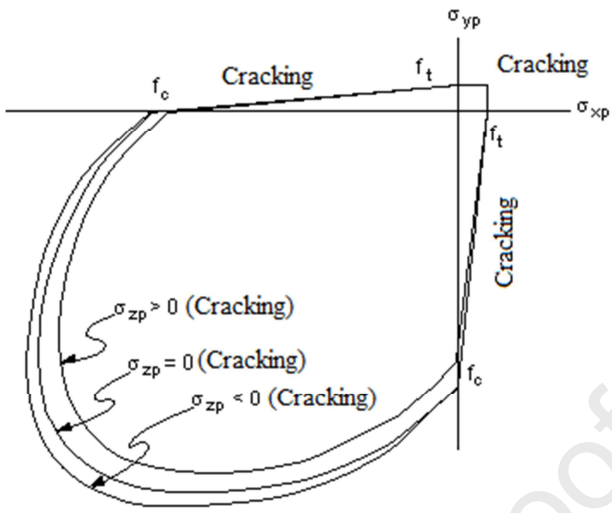

Fig.17 Surface of Failure in Biaxial Stress Space [42]

4.5. Constitutive Modelling of Steel Reinforcement

Bilinear stress-strain curve is used to idealize the behavior of the steel bars. As shown in Fig. 18, the stress-strain curve consists of two straight branches; the first branch represents the ascending branch at which the steel strain (ε_s) and the steel stress (f_s) are linearly increased up to the yield strain (ε_y) and the yield stress (f_y) respectively. The modulus of elasticity for the steel reinforcement is denoted by (E_s). The relationship for the two straight lines is expressed through the following equations [43]:

$$f_s = E_s\, \varepsilon_s \qquad \varepsilon_s \leq \varepsilon_y \tag{8.a}$$

$$f_s = f_y + E_h\, (\varepsilon_s - \varepsilon_y) \qquad \varepsilon_s > \varepsilon_y \tag{8.b}$$

Where;

ε_u= the ultimate strain of the steel reinforcement = $10\varepsilon_y$;

f_u = the ultimate stress of the steel reinforcement corresponding to the ultimate strain ε_u ;

E_s = the modulus of elasticity of the reinforcing steel (2x10^5 MPa);

E_h = the modulus of elasticity at the second branch of the curve that describes the strain hardening region. E_h can be considered as [43]:

$$E_h = 0.1\, E_s \tag{9}$$

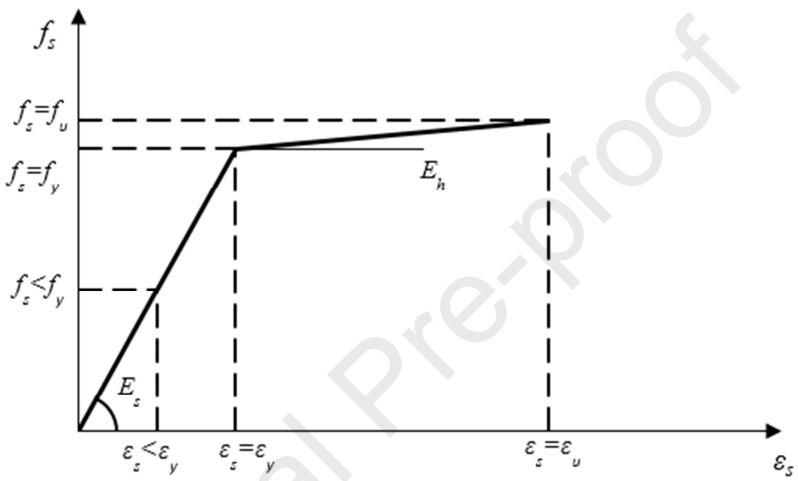

Fig.18 Bilinear Stress-Strain Curve for Steel Reinforcement [43]

4.6. Constitutive Modelling of GFRP Bars

The stress-strain curve for GFRP bars is shown in Fig.19. As shown in the figure, the stress-strain curve is linear till failure [44].

$$E_f = \frac{f_{fu}}{\varepsilon_{fu}} \tag{10}$$

Where:

f_{fu} = the ultimate tensile strength of GFRP bars;

ε_{fu} = the ultimate tensile strain of GFRP bars;

E_f = the modulus of elasticity of GFRP bars.

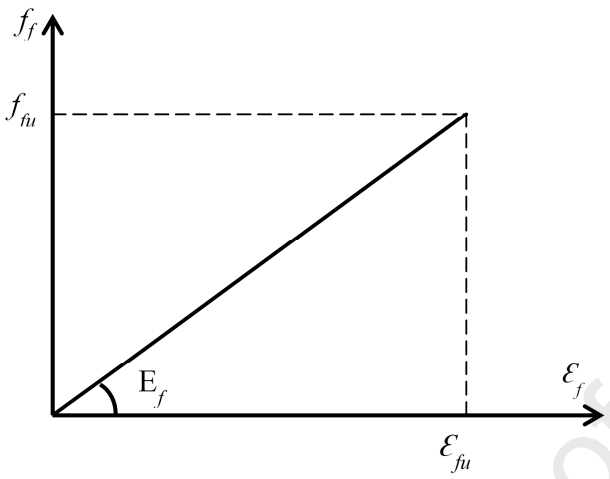

Fig. 19 Stress-Strain Curve for GFRP Bars [44]

Meshing of specimens has been performed according two concepts including; first according to the location of reinforcement whether main reinforcement mesh or vertical shear reinforcement where the intersection between them to ensure of the integration between concrete element and reinforcement bars where the nodes compatibility equations working correctly, secondly according to the concrete element boundary as such at the intersection between the slab and steel plates as shown in Fig. 20. The interface between steel bars, steel plates, GFRB bars and concrete was considered full bond in the model.

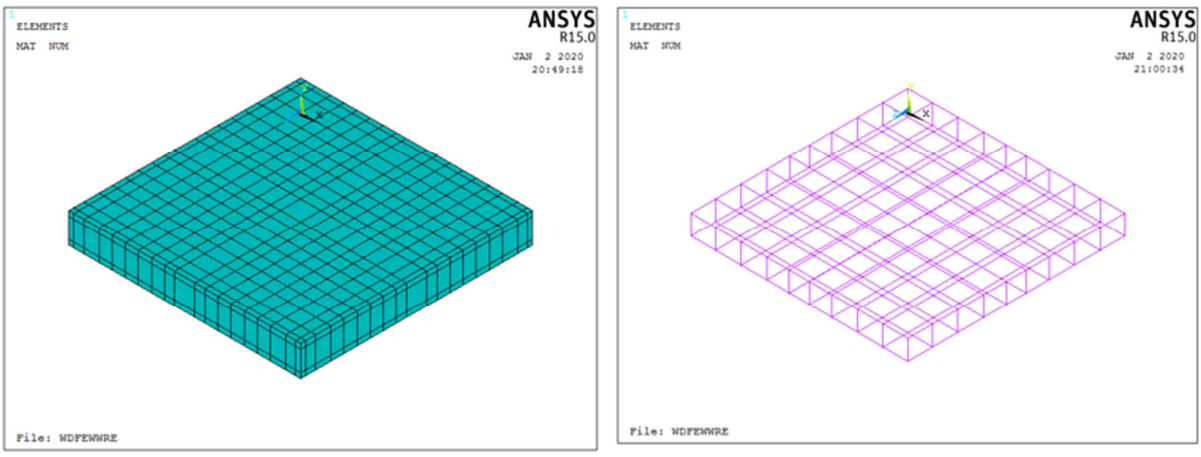

(a) Concrete element (Solid 65) **(b) Steel bar element (Link 180)**

Journal Pre-proof

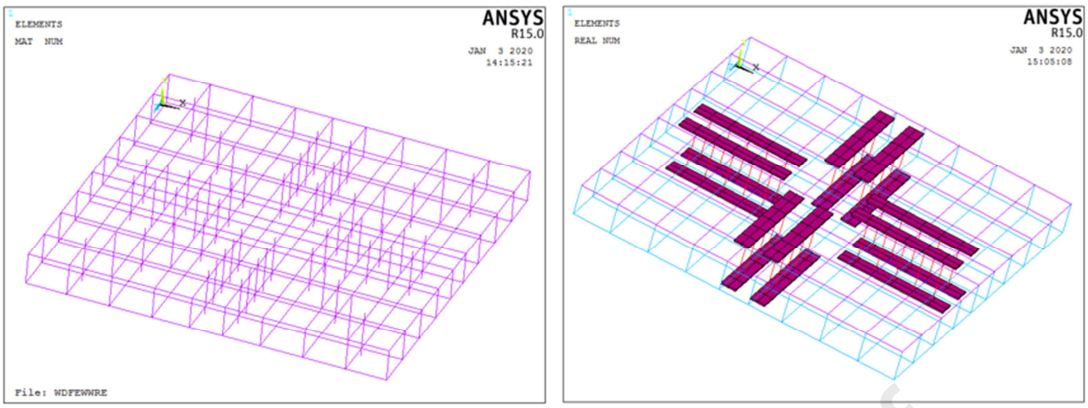

(c) Shear studs **(d) Shear studs with Steel Plates**

Fig.20 Finite Element Simulation Models for the Tested Specimens

4.7. NLFEA Model Verification

NLFEA results were verified with the experimental test results. All specimens almost have the same failure behavior due to the brittle and sudden failure occur. The predicted crack pattern is presented in Fig.21. Good agreements were achieved between the experimental and the numerical models. Generally, the load-deflection curves for the tested specimens displayed similar features. Comparison of the load-deflection curves extracted from ANSYS and test results for all specimens are plotted in Figs. 22 and listed in Table 5.

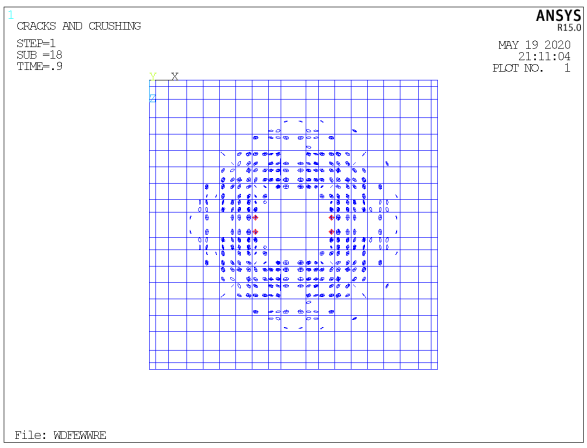

Specimen S1

Journal Pre-proof

Journal Pre-proof

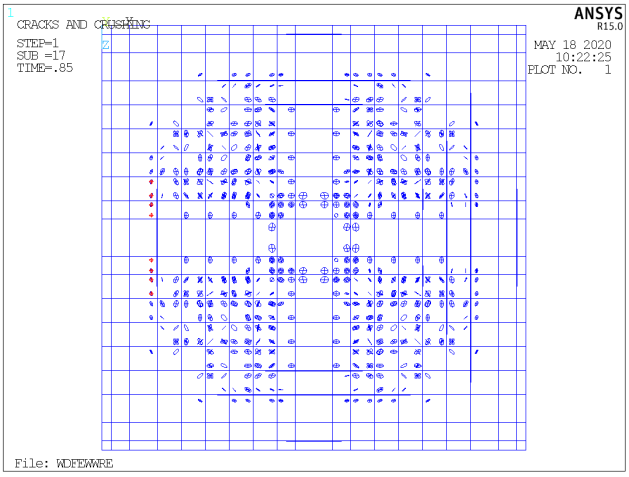

Specimen S2

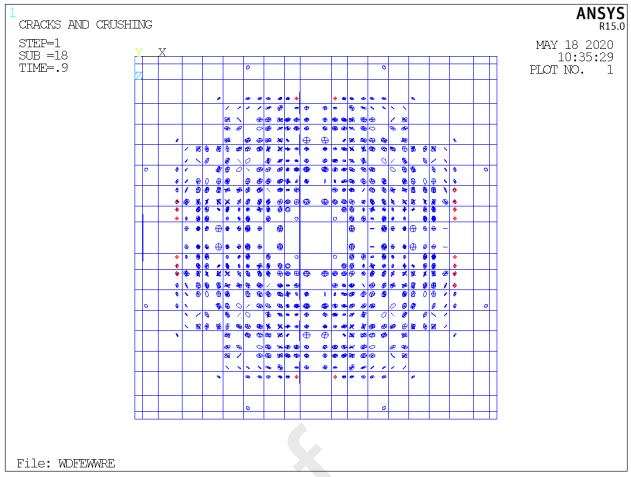

Specimen S3

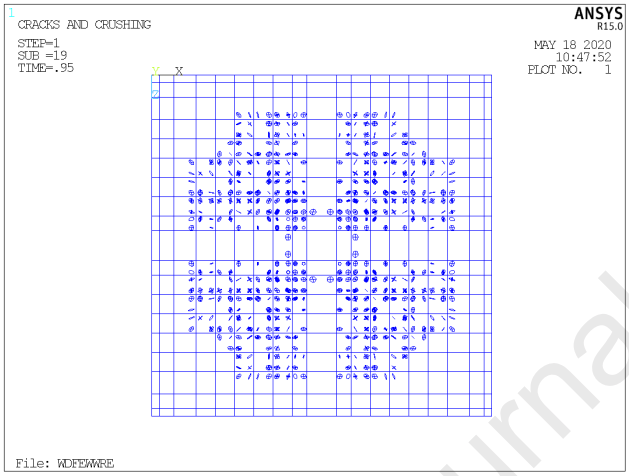

Specimen S4

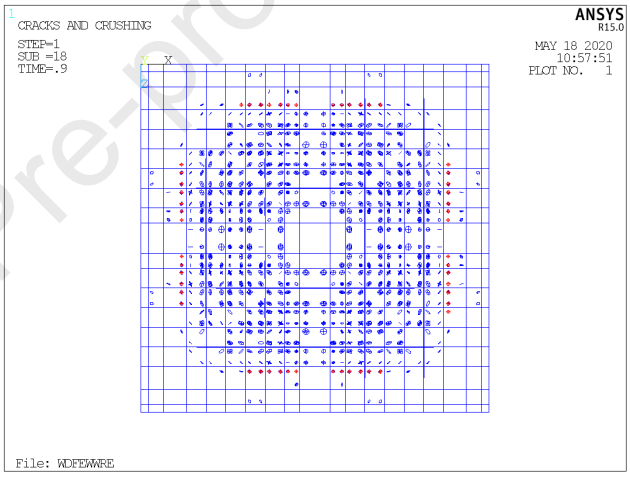

Specimen S5

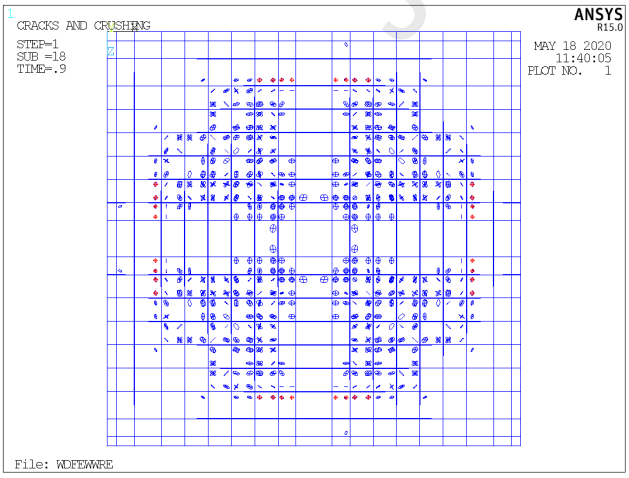

Specimen S6

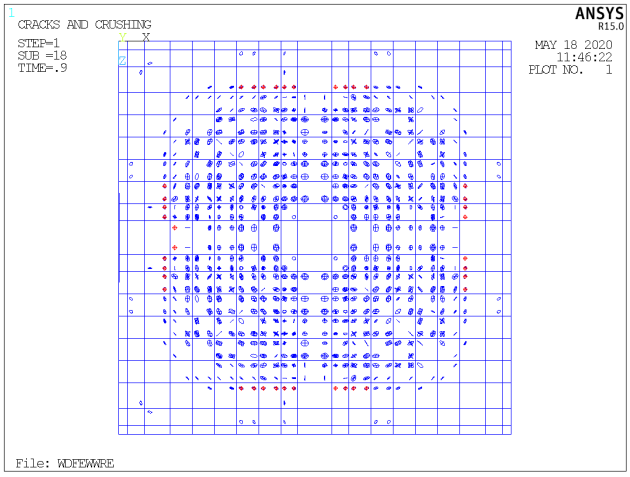

Specimen S7

Journal Pre-proof

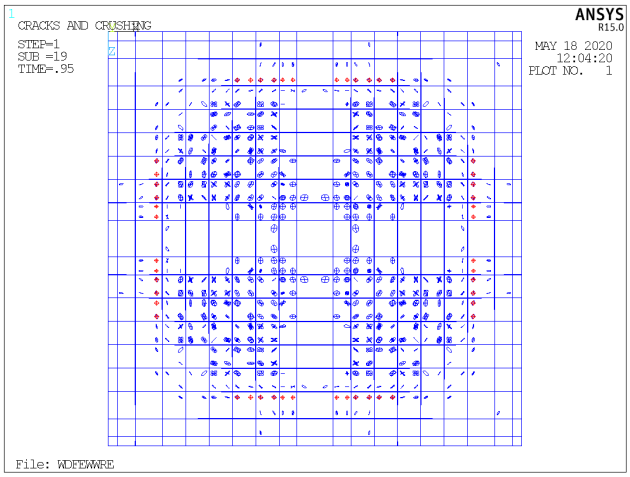

Specimen S8

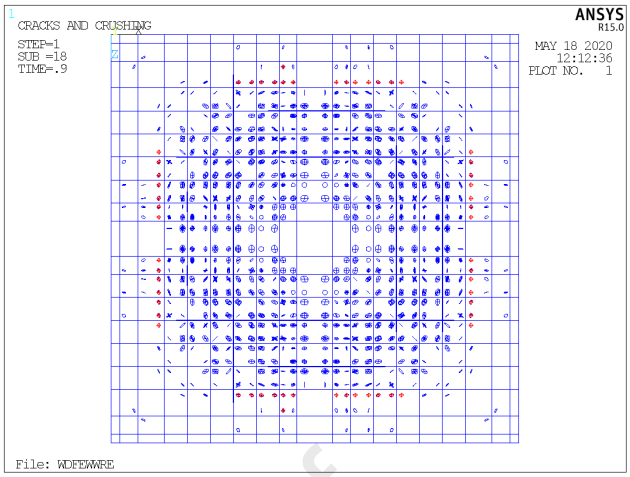

Specimen S9

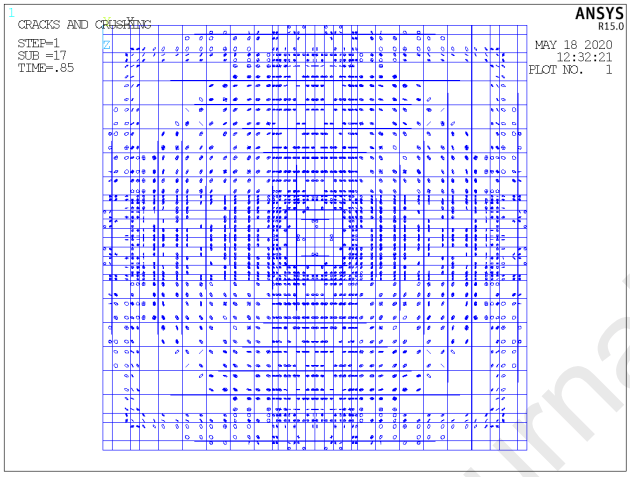

Specimen S10

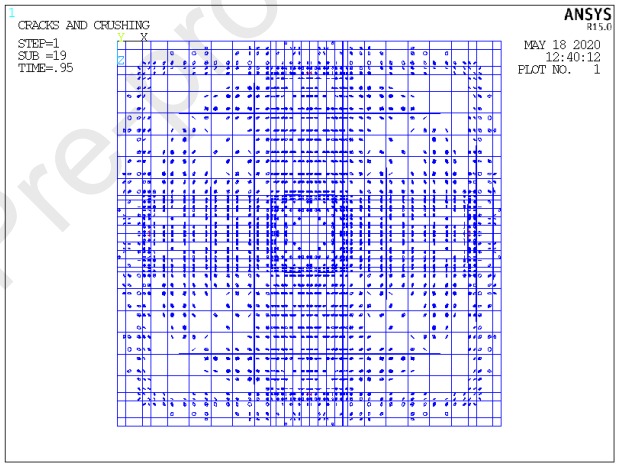

Specimen S11

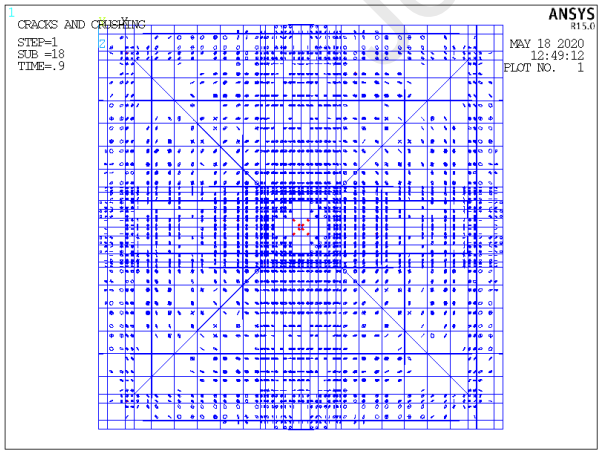

Specimen S12

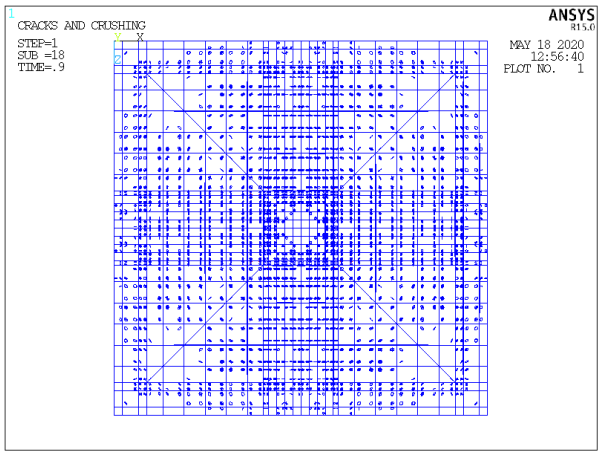

Specimen S13

Fig. 21 Predicted Cracks Propagation for Specimens

Journal Pre-proof

Journal Pre-proof

Table 5: Comparison of Experimental Results with NLFEA Results

Group	Specimen	Experimental Results			NLFEA Results			Experimental Results/ NLFEA Results		
		P_u (kN)	δ_u (mm)	I (kN.mm)	P_u (kN)	δ_u (mm)	I (kN.mm)	$\frac{P_{u-exp.}}{P_{u-NL.}}$	$\frac{\delta_{u-exp.}}{\delta_{u-NL.}}$	$\frac{I_{exp.}}{I_{NL.}}$
	S1	340	6.03	2191	370	5.9	1920	0.92	1.02	1.14
Group A	**S2**	576	13.2	8960	590	13	7350	0.98	1.02	1.22
	S3	523	11.75	6430	530	10	5851	0.99	1.18	1.10
	S4	603	9.95	5200	590	10.5	4561	1.02	0.95	1.14
	S5	539	10.5	6440	620	9.50	5552	0.87	1.11	1.16
Group B	**S6**	517	11.25	6320	550	11.2	5814	0.94	1.00	1.09
	S7	480	10.15	4840	520	9.8	4308	0.92	1.04	1.12
	S8	546	11.23	5650	570	9.05	4746	0.96	1.24	1.19
	S9	504	9.18	4260	530	9.5	3962	0.95	0.97	1.08
Group C	**S10**	473	11.14	27300	440	12.8	24570	1.08	0.87	1.11
	S11	412	10.27	18500	460	10.1	16095	0.90	1.02	1.15
	S12	522	18.3	33780	560	15.8	31111	0.93	1.16	1.09
	S13	476	15.35	30300	500	16.9	26664	0.95	0.91	1.14
Average								**0.95**	**1.04**	**1.13**
Standard deviation								**0.05**	**0.11**	**0.07**
Coefficient of variation								**6%**	**10%**	**6%**

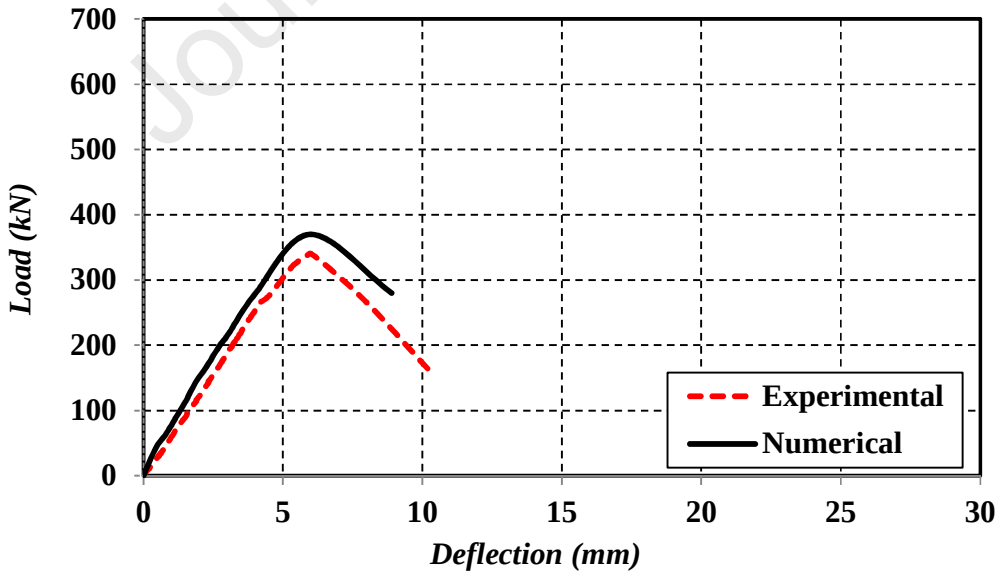

S1

Journal Pre-proof

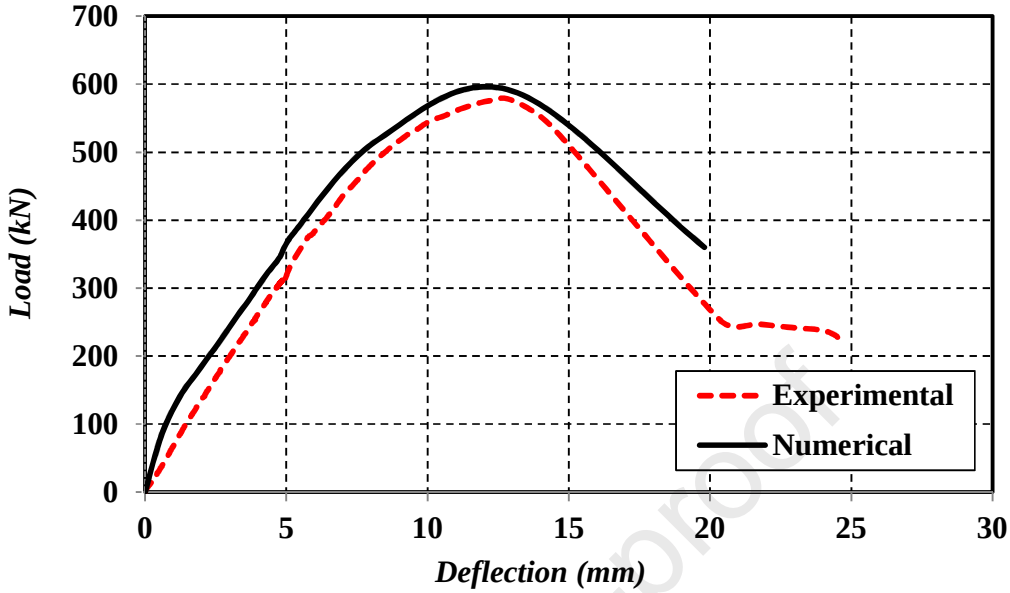

S2

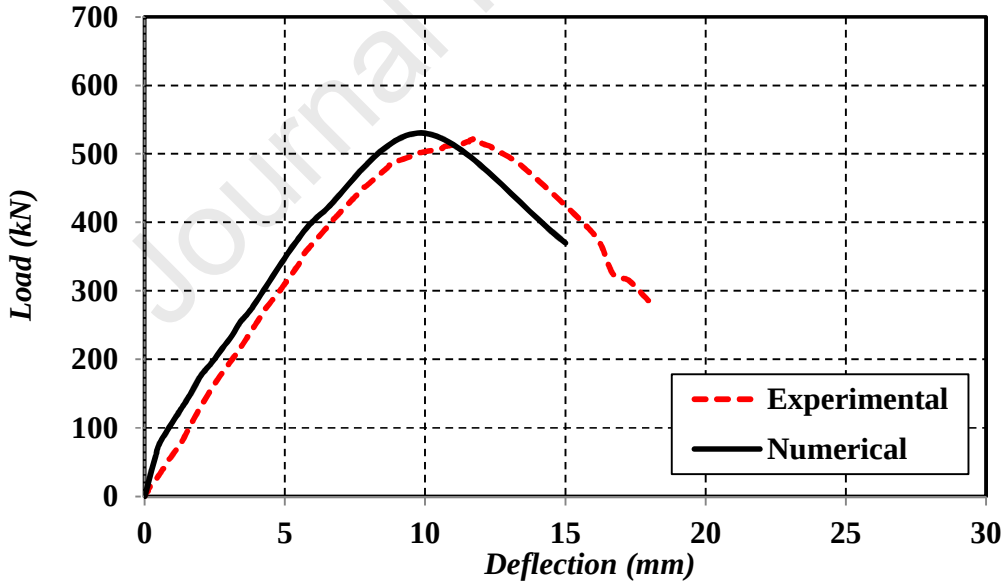

S3

Journal Pre-proof

Journal Pre-proof

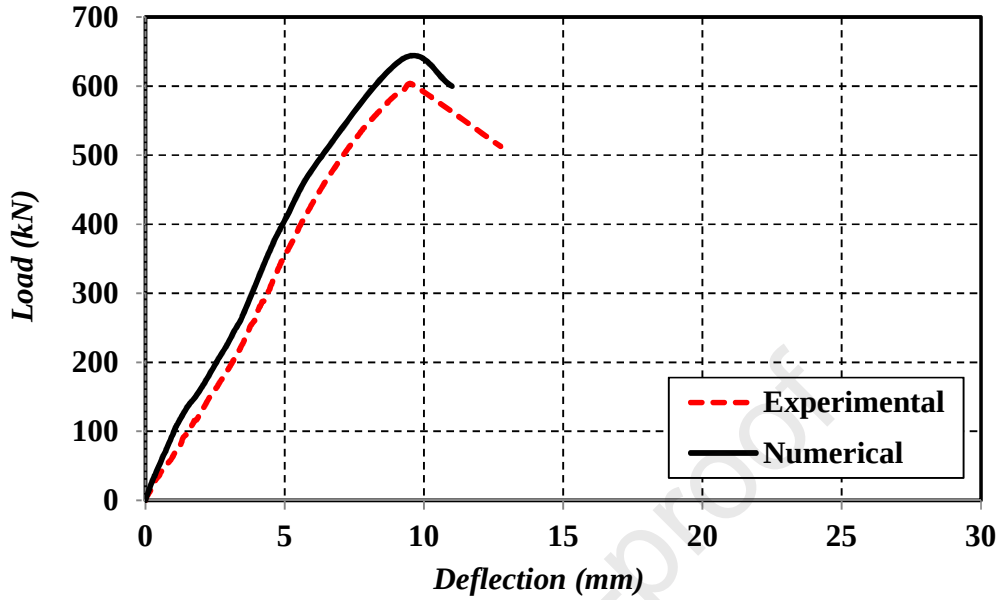

S4

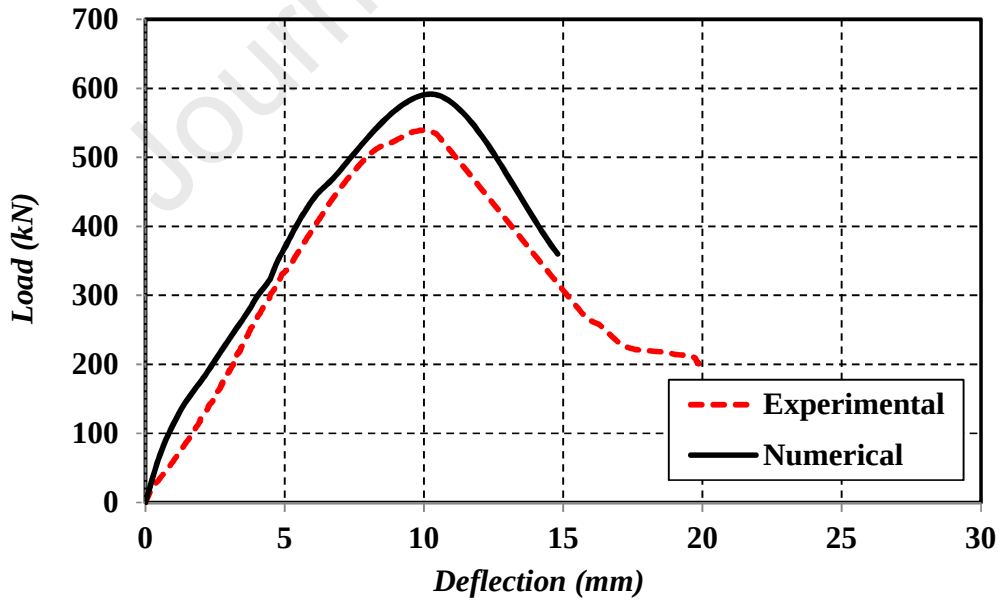

S5

Journal Pre-proof

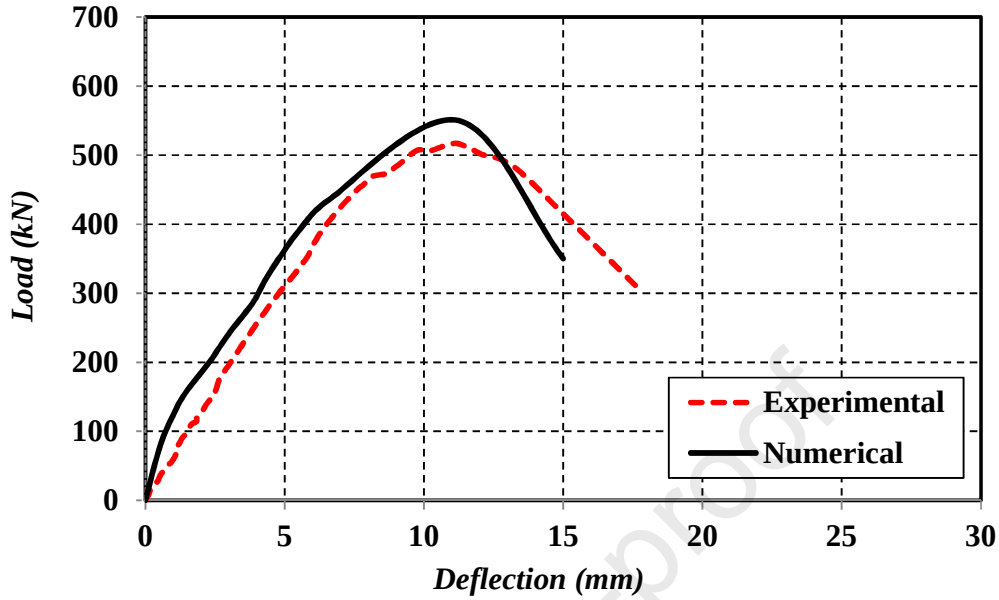

S6

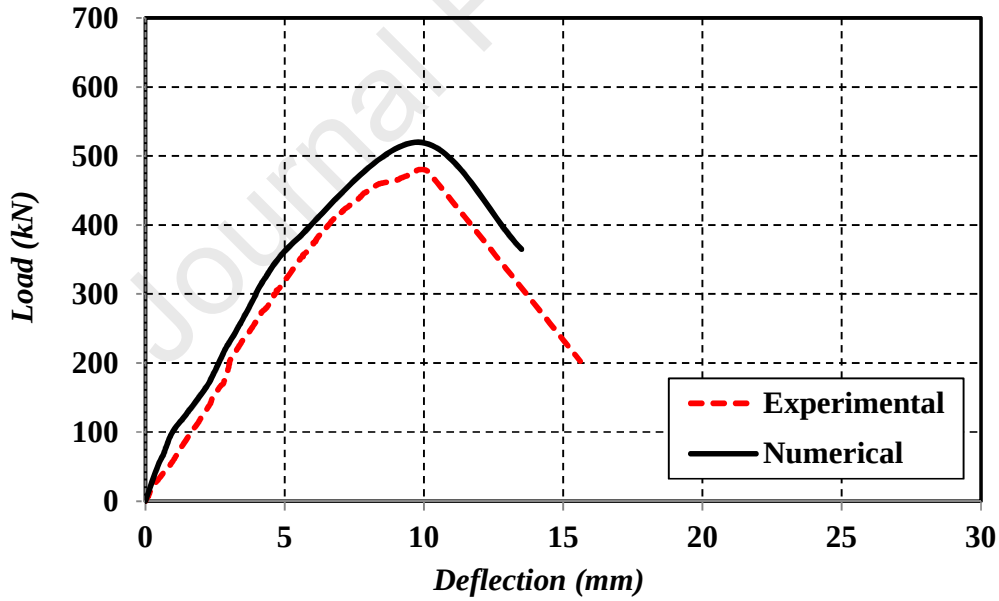

S7

Journal Pre-proof

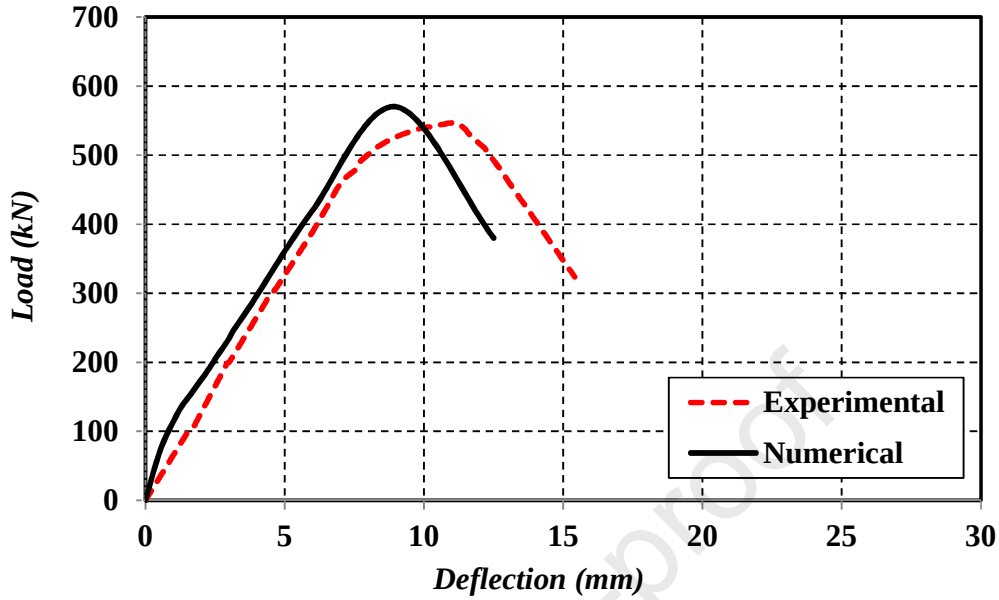

S8

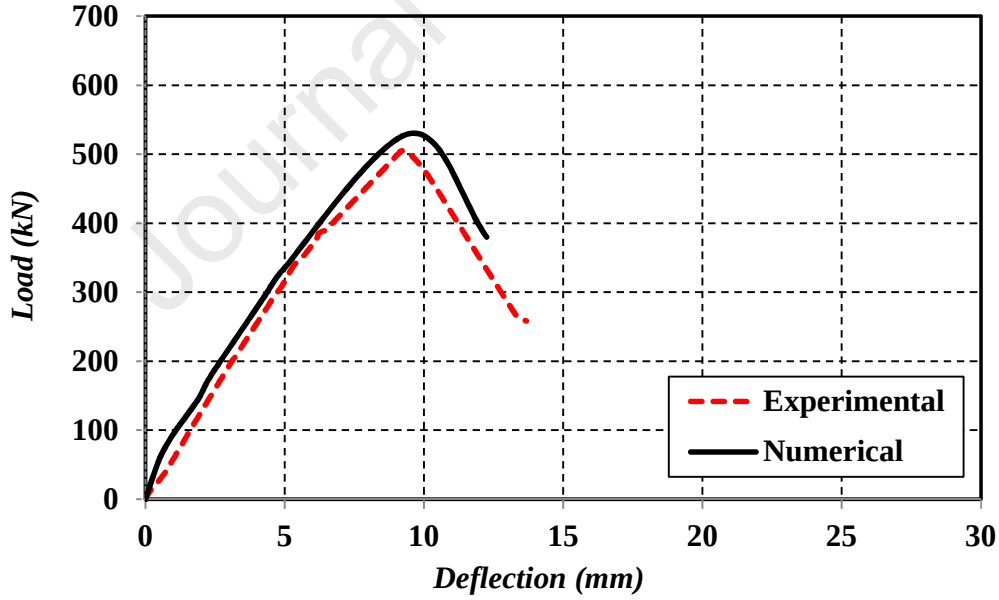

S9

Journal Pre-proof

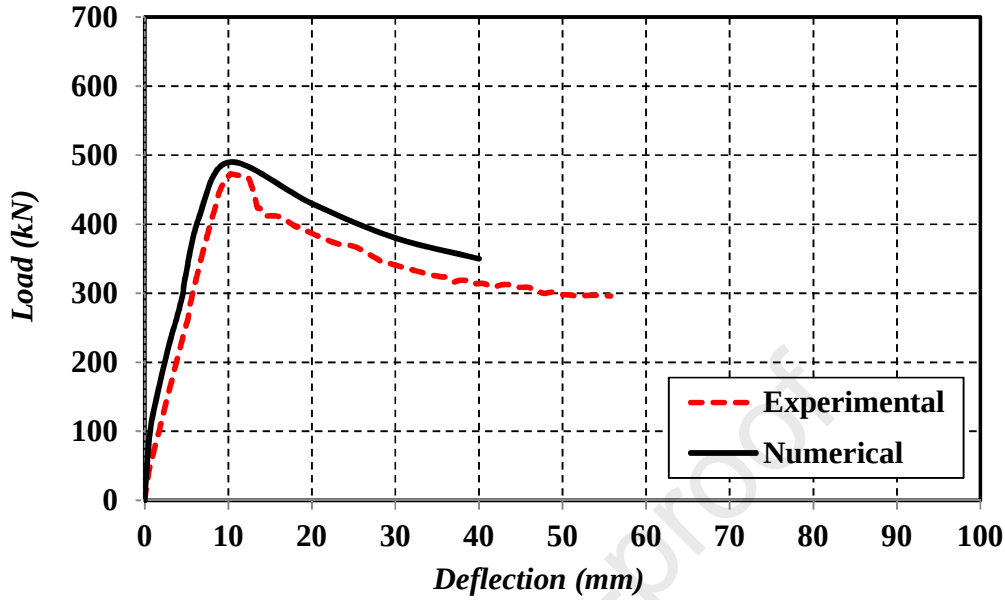

S10

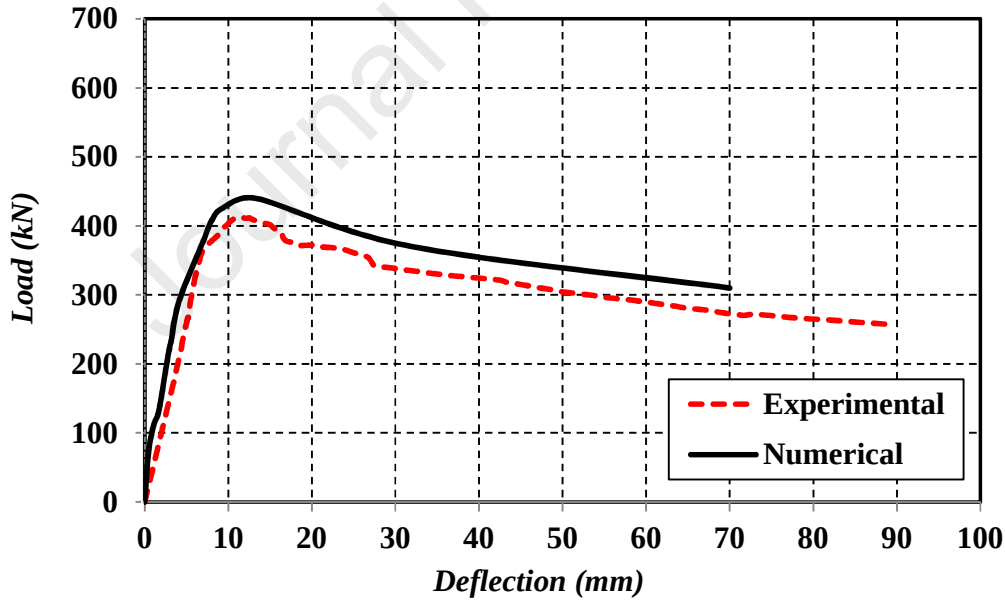

S11

Journal Pre-proof

Journal Pre-proof

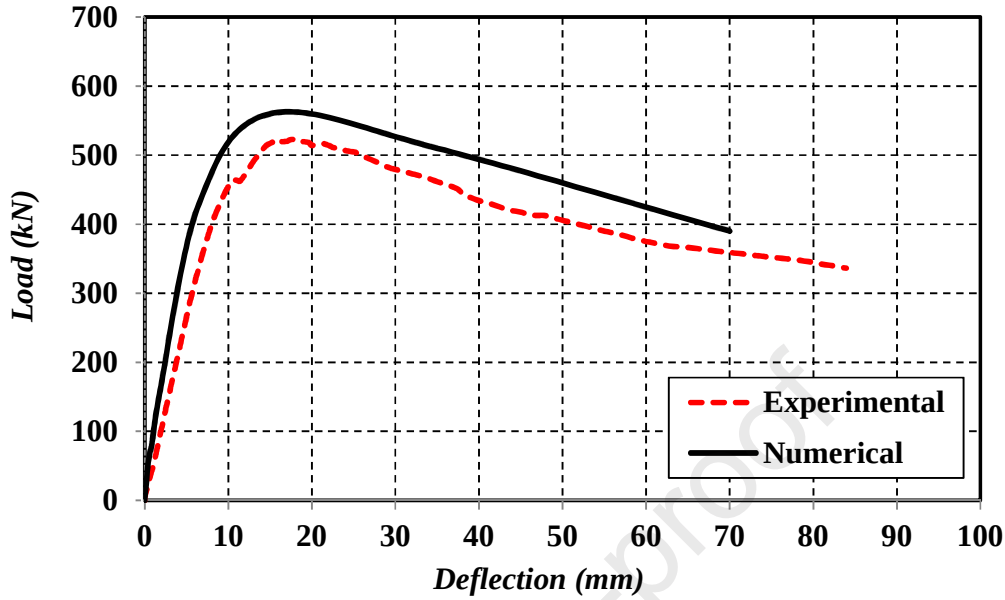

S12

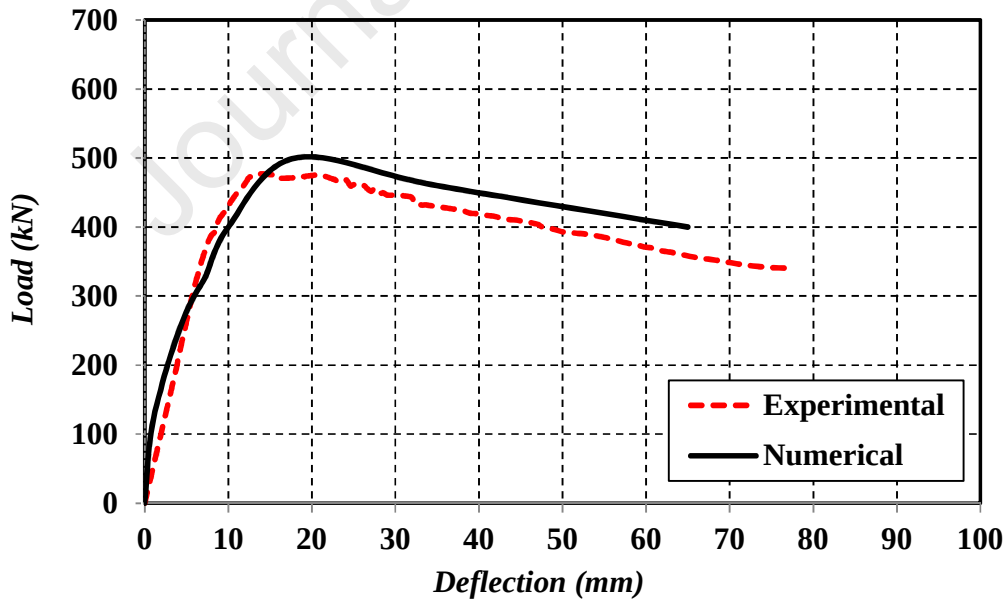

S13

Fig.22 Comparison of Predicted Deflections with Experimental Values

Journal Pre-proof

Journal Pre-proof

5. Building Codes Evaluation

The experimental test results were compared with the design codes. The used design codes were ACI-318-18 [35], CSA A23.3-2004 [36], ECP-203-2017 [37], BS-8110-1997 [38] and EC-2- EN 1992-1-1 [39].Commonly, the design codes define the punching shear strength as the product of the design nominal shear strength of concrete and the area of the chosen critical section. Depending on the code used, the critical section for predicting punching shear strength in slabs should be between the column face and a distance up to 2d. Table 6 presents a comparison between the experimental test results and the punching shear strength calculations by different codes for all specimens. The calculation of the punching shear strength is predicted at distance 0.5d from the loaded plate face. Table 6 indicates a significant variation in the punching shear predictions from a certain code to another. The overall average ($P_{u,Code}/P_{u,Exp.}$) is ranged from 0.56 to 0.99 with a coefficient of variation (C.O.V) ranging from 9.9% to 13%. ACI 318-2018 [35] underestimated the punching shear capacity of the tested slabs with an average ($P_{u,\,ACI}\,/P_{u,\,Exp.}$) of 0.56. CSA A23.3-2004 [36] underestimated the punching shear capacity of the tested slabs with an average of 0.70. BS-8110-1997 [38] underestimated the punching shear capacity of the tested slabs with an average of 0.80. ECP-203-2017 [37] underestimated the punching shear capacity of the tested slabs with an average of 0.60. On the other hand, EC-2- EN 1992-1-1 [39] showed good prediction of the punching shear strength of the tested slabs with an overall average ($P_{u,\,EC2}\,/P_{u,\,Exp.}$) of 0.99.

Journal Pre-proof

Table 6: Comparison between Design Codes

Sp.	$P_{u,Exp}(kN)$	Predicted ultimate load ; P_u (kN)									
		$P_{u,ACI}(kN)$	$P_{u,CSA}(kN)$	$P_{u,ECP}(kN)$	$P_{u,BS}(kN)$	$P_{u,EC2}(kN)$	$\frac{P_{u,ACI}}{P_{u,Exp.}}$	$\frac{P_{u,CSA}}{P_{u,Exp.}}$	$\frac{P_{u,ECP}}{P_{u,Exp.}}$	$\frac{P_{u,BS}}{P_{u,Exp.}}$	$\frac{P_{u,EC2}}{P_{u,Exp.}}$
S1	340	243	181.9	212.8	207	256	0.71	0.54	0.63	0.61	0.75
S2	576	276	358.8	302.4	414	512	0.48	0.62	0.53	0.72	0.89
S3	523	276	358.8	302.4	414	512	0.53	0.69	0.58	0.79	0.98
S4	603	276	358.8	302.4	414	512	0.46	0.60	0.50	0.69	0.85
S5	539	276	358.8	302.4	414	512	0.51	0.67	0.56	0.77	0.95
S6	517	276	358.8	302.4	414	512	0.53	0.69	0.58	0.80	0.99
S7	480	276	358.8	302.4	414	512	0.58	0.75	0.63	0.86	1.07
S8	546	276	358.8	302.4	414	512	0.51	0.66	0.55	0.76	0.94
S9	504	276	358.8	302.4	414	512	0.55	0.71	0.60	0.82	1.02
S10	412	276	358.8	302.4	414	512	0.67	0.87	0.73	1.01	1.24
S11	473	276	358.8	302.4	414	512	0.58	0.76	0.64	0.88	1.08
S12	522	276	358.8	302.4	414	512	0.53	0.69	0.58	0.79	0.98
S13	476	276	358.8	302.4	414	512	0.58	0.75	0.64	0.87	1.08
Average							0.56	0.69	0.60	0.80	0.99
Standard deviation							0.072	0.084	0.059	0.098	0.121
Coefficient of variation							12.95%	12.14%	9.95%	12.32%	12.32%

Journal Pre-proof

6. Conclusion

The strengthening techniques of reinforced LWC slabs under punching shear were investigated. Based on the experimental results and the comparison with the NLFEA in this study, the main conclusions can be drawn as follows:

1. Generally, all strengthening techniques displayed an enhancement in the punching shear capacity for all specimens compared with the control specimen without shear reinforcement. The absence of the shear reinforcement for the reference specimen led to the brittle failure mode.

2. Using steel bars studs as shear reinforcement showed a significant enhancement in the punching shear strength, the capacities were improved by 69%, 54%, 77% and 59% compared with the reference specimen.
3. The inclusion of GFRP rods as shear reinforcement improves the punching shear capacity of the specimens compared with the control slab. However, due to the low stiffness and modulus of elasticity of GFRP bars, the enhancement values were less than the steel bars strengthening techniques. The punching shear capacity was enhanced by 52%, 41%, 61% and 48%.
4. Provision of high strength steel bolts fixed to the slabs with steel plates as a strengthening technique enhanced the punching load capacity compared to control slab. Moreover, a noticeable ductile behaviour after peak load was observed comparing with the other specimens. In addition, the failure mode converted from being brittle shear failure to shear-flexural failure.
5. Utmost enhancement in the ductility was achieved for specimens strengthened using high strength steel bolts with steel plates.
6. Generally, using radial reinforcement spaced with 0.5d was the most efficient strengthening technique to enhance the punching shear strength of LWC flat slabs.
7. Application of NLFEA to the tested specimens, yielded acceptable prediction of load-carrying capacities, and load-deflection curves. The analysis adequately reflected the trend of experimental results. At ultimate level, the overall average ratio [$P_{u,\,exp.}$ / $P_{u,\,NL.}$] was 0.95 with a standard deviation of 0.05 and coefficient of variation equal 6%.
8. Evaluation of the experimental test results with the design codes showed that ACI 318-2018 code underestimated the punching shear strength; the average ($P_{u,\,ACI}$ /$P_{u,\,Exp.}$) was

Journal Pre-proof

0.56. On the other hand, EC-2- EN 1992-1-1 showed good prediction of the punching shear strength of the tested slabs with an overall average (Pu, EC2 / Pu, Exp.) of 0.99.

Declaration of Competing Interest

The authors declare that they have no known competing financial interests or personal relationships that could have appeared to influence the work reported in this paper.

References

1. Wu, X., Yu, S., Xue, S., Kang, T. H. K., Hwang, H. j., "Punching Shear Strength of UHPFRC-RC Composite Flat Plates", Engineering Structures, Vol.184, pp. 278-286, 2019.

2. Baniya, W. J., Zaki, W., Farrag, C. R., Rashed, D. A., "Behavior of Composite Pre-Flat Slabs in Resisting Punching Shear Forces", Alexandria Engineering Journal, Vol.42, pp.1-15, 2020.

3. Muttoni, A., "Punching Shear Strength of Reinforced Concrete Slabs without Transverse Reinforcement", ACI Structural Journal, Vol.105, pp.440-450, 2008.

4. Sacramento, P., Ferreira, M., Oliveira, D. R. C., Melo, G. S. S. A., "Punching Strength of Reinforced Concrete Flat Slabs without Shear Reinforcement", IBRACON, Vol.5, pp.659-691, 2012.

5. Dan, V. B., Onet, T., "Punching Shear Strength of RC Flat Slabs at Interior Connections to Columns", Magazine of Concrete Research, Vol.68, pp.24-42, 2016.

6. Cui, H. Z., Lo, T. Y., Memon, S. A., Xing, F., Shi, X., "Analytical Model for Compressive Strength, Elastic Modulus and Peak Strain of Structural Lightweight Aggregate Concrete", Construction and Building materials, Vol.36, pp.1036-1043, 2012.

7. Go, C.G., Tang, J.R., Chi, J. H., Chen, C. T., Huang, Y. L., "Fire-Resistance Property of Reinforced Lightweight Aggregate Concrete Wall", Construction and Building Materials, Vol.30, pp.725-733, 2012.

Journal Pre-proof

8. Kim, H. K., Jeon, J. H., Lee, H. K., "Workability, Mechanical Acoustic and Thermal Properties of Lightweight Aggregate Concrete with a High Volume of Entrained Air", Construction and Building Materials, Vol.29, pp.193-200, 2012.

9. Costa, H., Júlio, E., Lourenco, J., "New Approach for Shrinkage Prediction of High-Strength Lightweight Aggregate Concrete", Construction and Building Materials, Vol.35, pp.84-91, 2012.

10. Chung, S. Y., Han, T. S., Yun, T. S., Youm, K. S., "Evaluation of the Anisotropy of the Void Distribution and the Stiffness of Lightweight Aggregates using CT Imaging", Construction and Building Materials, Vol. 48, pp.998-1008, 2013.

11. Khaleel, G., Shaaban, I., Elsayedand, K. M., Makhlouf, M. H., "Strengthening of Reinforced Concrete Slab-Column Connection subjected to Punching Shear with FRP Systems", International Journal of Engineering and Technology, Vol.5, pp.657-661, 2013.

12. Saleh, H., Kalfat, R., Abdouka, K., Al-Mahaidi, R., "Punching Shear Strengthening of RC Slabs using L-CFRP Laminates", Engineering Structures, Vol.194, pp.274-289, 2019.

13. Wiater, A., Tomasz, S., "Serviceability and Ultimate Behaviour of GFRP Reinforced Lightweight Concrete Slabs" Experimental Test versus Code Prediction", Composite Structures, Vol.19, 2020.

14. Shaaban, I., Said, M., "Effect of Partial Replacement of Coarse Aggregate by Polystyrene Balls on the Shear Behaviour of Deep Beams with Web Openings", Case Studies in Construction Materials, Vol.12, pp.1-26, 2020.

15. Zaher, A. A., Abdelrahman, A. A., Eldeib, A. S., Mohamed, A. A., "Punching Shear Behavior of Lightweight Foamed RC Slabs", International Journal of Application or Innovation in Engineering & Management, Vol.4, pp.67-74, 2015.

16. Youm, K. S., Jeon, H. K., Park, Y. S., Lee, S. H., Moon, J., "Experimental Study on Punching Shear of Lightweight Concrete Slab", Proceedings of the Thirteenth East Asia-Pacific Conference on Structural Engineering and Construction (EASEC-13), September 11-13, 2013, Sapporo, Japan.

Journal Pre-proof

17. Caratelli, A., Imperatore, S., Meda, A., Rinaldi, Z., “Punching Shear Behavior of Lightweight Fiber Reinforced Concrete Slabs”, Composites Part B: Engineering, Vol.99, pp. 257-265, 2016.

18. Urban, T., Gołdyn, M., Krawczyk, L., Sowa, L., “Experimental Investigations on Punching Shear of Lightweight Aggregate Concrete Flat Slabs”, Engineering Structures, Vol.64, pp. 293-306, 2019.

19. Cho, S. K., Kwark, J. W., Lee, J. M., Moon, D. J., “Punching Shear Behavior of High-Strength Lightweight Concrete Slab under Concentrated Load”, Journal of the Korean Society of Civil Engineers, Vol.26, pp.219-228, 2006.

20. McLean, D. I., Phan, L. T., White, R. N., “Punching Shear Behavior of Lightweight Concrete Slabs and Shells”, Structural Journal, Vol.87, pp.386-392, 1990.

21. Marzouk, H., Osman, M., Helmy, S., “Behavior of High-Strength Lightweight Aggregate Concrete Slabs under Column Load and Unbalanced Moment”, Structural Journal, Vol.97, pp.860-866, 2000.

22. Aghayari, R., Moradi, M., “Improving the Punching Shear Strength of RC Slabs by FRP and Steel Sheets”, Journal of Rehabilitation in Civil Engineering, V. 4, Issue 1, pp. 1-17. 2016.

23. Lapi, M., Ramos, A. P., Orlando, M., “Flat Slab Strengthening Techniques against Punching-Shear”, Engineering Structures, V.180, pp.160–180, 2019.

24. El-Kashif, K. F., Ahmed, E. A., Salem, H. M., “Experimental Investigation of Strengthening Slab-Column Connections with CFRP Fan”, Ain Shams Engineering Journal, Vol.10, pp.639-650, 2019.

25. Silva, M. A., Gamage, J. C. P., Fawzia, S., “Performance of Slab-Column Connections of Flat Slabs Strengthened with Carbon Fiber Reinforced Polymers”, Case Studies in Construction Materials, Vol.11, pp.1-9, 2019.

Journal Pre-proof

26. El-Esnawi, H., “Strengthening of Interior Slab Column Connections via Post Installed Steel Shear Bolts”, Journal of Al-Azhar University Engineering Sector, Vo.13, pp.988-996, 2018.

27. Hamdy, M., Saafan, M., Elwan, S. K., Elzeiny, S., Abdelrahman, A., “Punching Shear Behavior of RC Flat Slabs Strengthened with Steel Shear Bolts”, International Journal of Current Engineering and Technology, Vol.8, pp.651-663, 2018.

28. Akhundzada, H., Donchev, T., Petkova, D., “Strengthening of Slab-Column Connection against Punching Shear Failure with CFRP Laminates”, Composite Structures, Vol.208, pp.1-19, 2018.

29. Santos, G. S., Melo, G. S. A., Barros, J. O., “Punching CFRP-Based Strengthening Solutions for Reinforced Concrete Flat Slabs”, Composite Structures, Vo.224, pp.1-18, 2019.

30. Saleh, H., Kalfat, R., Abdouka, K., Al-Mahaidi. R., “Experimental and Numerical Study into the Punching Shear Strengthening of RC Flat Slabs using Post-Installed Steel Bolts”, Construction and Building Materials, Vol.188, pp.28-39, 2018.

31. Genikomsou, A., Polak, M. A., “Finite Element Simulation of Concrete Slabs with various Placement and Amount of Shear Bolts”, Procedia Engineering, Vol.193, pp.313–320, 2017.

32. Kadam, K., Shaikh, V., “Behaviour of Flat Slab a Study by Finite Element Analysis”, International Journal of Innovative Research in Science, Vol.7, pp.2213–2218, 2018.

33. Navarro, M., Ivorra, S., “Parametric Finite Element Analysis of Punching Shear Behavior of RC Slabs Reinforced with Bolts”, Engineering Structures, Vol.63, pp.165:254, 2019.

34. ANSYS–Release Version 15.0, “A Finite Element Computer Software and User Manual for Nonlinear Structural Analysis”, ANSYS Inc. Canonsburg, PA., (2009).

35. ACI Committee 318, (2018), “Building Code Requirements for Structural Concrete (ACI 318-18)”, American Concrete Institute, Farmington Hills, Mich.

Journal Pre-proof

36. Canadian Standards Association, (2004), “Design of Concrete Structures for Buildings”, (CSA, A23.3-2004), Rexdale, Ontario, Canada.

37. Egyptian code of practice for design and construction of reinforced concrete structures (ECP-203-2017), (2017), Housing and Building Research Center, Giza, Egypt.

38. British Standards Institution, (1997), “Structural Use of Concrete, BS8110: Part 1-Code of Practice for Design and Construction,” London.

39. EC-2, (2004), “Eurocode 2: Design of Concrete Structures—Part 1: General Rules and Rules for Buildings,” European Prestandard EN 1992-1-1:2004(E).

40. Montoya, E., Vecchio, F., Sheikh, S.A., “Compression Field Modelling of Confined Concrete”, Journal of Structural Engineering and Mechanics, Vol.12, No.3, (2001).

41. Careira, D. J., Chu, K. H., ‘‘Stress-Strain Relationship of Reinforced Concrete in Tension’’, ACI Materials Journal, Vol.83, pp.21-28, 1990.

42. Willam, K.J., Warnke, E. P., “Constitutive Model for Triaxial Behavior of Concrete”, Seminar on Concrete Structures Subjected to Triaxial Stresses, International Association of Bridge and Structural Engineering Conference, Bergamo, Italy, 174, 1974.

43. Eurocode 3, “Design of Steel Structures, ENV EC3 Part 1.2.", Eurocode, (2005).

44. American Concrete Institute (ACI), “Guide for the Design and Construction of Concrete Reinforced with FRP Bars”, ACI 440.1R-03, ACI Committee 440, Farmington Hills, Michigan, 2003.

Journal Pre-proof

Journal Pre-proof

Highlights

- Strengthening techniques showed an improvement in the punching shear strength of the specimens.
- Using diagonal shear reinforcement considered one the most effective ways for strengthening of LWC flat slabs.
- Radial reinforcement spaced with 0.5d was the most efficient strengthening technique to enhance the punching shear strength of LWC flat slabs.
- Strengthening with GFRP rods as shear reinforcement improves the punching shear capacity.
- Utmost enhancement in the ductility was achieved for specimens strengthened using high strength steel bolts with steel plates.

Journal Pre-proof

Journal Pre-proof

Disclosure Statement

Dear Editor;

I wish to confirm that there are no known conflicts of interest associated with this publication and there has been no significant financial support for this work that could have influenced its outcome.

I confirm that the manuscript has been read and approved by all named authors and that there are no other persons who satisfied the criteria for authorship but are not listed. I further confirm that the order of authors listed in the manuscript has been approved by all of authors.

I confirm that we have given due consideration to the protection of intellectual property associated with this work and that there are no impediments to publication, including the timing of publication, with respect to intellectual property. In so doing I confirm that I have followed the regulations of our institutions concerning intellectual property.

Sincerely,

Mohamed Said
Associate Professor
Department of Civil Engineering, Faculty of Engineering, Benha University, 108 Shoubra St., Shoubra, Cairo, Egypt
Tel.: +2 01007284649, E-mail: Mohamed.abdelghaffar@feng.bu.edu.eg

Journal Pre-proof